ENCYCLOPEDIA OF VOLCANOES (3RD EDITION)

PART 2: Terrestrial and Extra-Terrestrial Volcanic Environments

Section 2: Terrestrial Environments – Tectonic Settings

CHAPTER 2.3: ‘Mid-Ocean Ridge Volcanism’

William W. Chadwick Jr.[1], Mathilde Cannat[2], Deborah Eason[3],
Morgane Le Saout[4], Rebecca J. Carey[5]

1 – Oregon State University, CIMERS, Hatfield Marine Science Center, Newport, OR, USA
2 – Marine Geosciences, Institut de Physique du Globe de Paris, Paris, France
3 – Department of Earth Sciences, SOEST, University of Hawaiʻi at Mānoa, Honolulu, HI, USA
4 – Department of Earth Sciences, University of Bergen, Bergen, Norway
5 – CODES, School of Natural Sciences, University of Tasmania, Australia

This is a peer-reviewed preprint submitted to EarthArXiv. The manuscript is a Chapter of forthcoming book: The Encyclopedia of Volcanoes, 3rd ed. Editors: C. Bonadonna, L. Caricchi, A. Clarke, P. Cole, J. Lindsay, J. Lowenstern, R. Robertson and M. L. Villegas, that will be published by Elsevier. As one of the first 20 chapters to be accepted for publication in the book, it is being allowed to be submitted to *EarthArXiv* as a preprint.

ENCYCLOPEDIA OF VOLCANOES (3RD EDITION)

PART 2: Terrestrial and Extra-Terrestrial Volcanic Environments

Section 2: Terrestrial Environments – Tectonic Settings

CHAPTER 2.3: ‘Mid-Ocean Ridge Volcanism’

William W. Chadwick Jr.[1], Mathilde Cannat[2], Deborah Eason[3],
Morgane Le Saout[4], Rebecca J. Carey[5]

1 – Oregon State University, CIMERS, Hatfield Marine Science Center, Newport, OR, USA
2 – Marine Geosciences, Institut de Physique du Globe de Paris, Paris, France
3 – Department of Earth Sciences, SOEST, University of Hawaiʻi at Mānoa, Honolulu, HI, USA
4 – Department of Earth Sciences, University of Bergen, Bergen, Norway
5 – CODES, School of Natural Sciences, University of Tasmania, Australia

Abstract

The vast majority of the Earth’s volcanism takes place in the deep ocean along mid-ocean ridges (MORs), yet because it is difficult to detect and observe, it is also relatively poorly understood. MOR volcanism occurs where tectonic plates spread apart and mainly produces effusive basaltic fissure eruptions where dikes reach the surface. The character and frequency of volcanism varies greatly as a function of spreading rate and magma supply, as does the morphology of the ridge crest, the balance between volcanic construction and tectonic faulting, and the scales of ridge segmentation. The depth and continuity of magma storage in the crust beneath MORs also depends greatly on the local magma supply in space and time. The generation of MOR magmas is ultimately due to partial melting processes in the mantle where it rises beneath ridges due to plate spreading.

Keyword lists: Spreading center, divergent plate boundary, ridge crest, neovolcanic zone, seafloor bathymetry, submarine eruption, pillow lava, magma supply, ocean crust, basalt

1. Introduction

It is estimated that ~75% of Earth’s volcanic output occurs along the 65,000-km long global mid-ocean ridge (MOR) system, making it the dominant expression of volcanism on the planet. Basaltic ocean crust formed at MORs is also the most common rock type on Earth’s surface, underlying the vast ocean basins that cover 71% of the planet (Fig. 1). Yet, MOR volcanism in the deep sea is also the most difficult and challenging form of volcanic activity to detect and observe, because it occurs under the veil of the oceans and far from monitoring networks on land. Even though many MOR eruptions likely occur on Earth every year, not a single historical eruption had been documented in the deep sea before 1991, when the first two were serendipitously discovered shortly after they had occurred [1]. Thus, MOR volcanism is not as well understood as volcanic activity on land, but our knowledge is growing rapidly thanks to recent research and technological advances (QR code #1).

Insert **QR code #1** here for online “How To” video: “How Do We Study Submarine Volcanoes?”

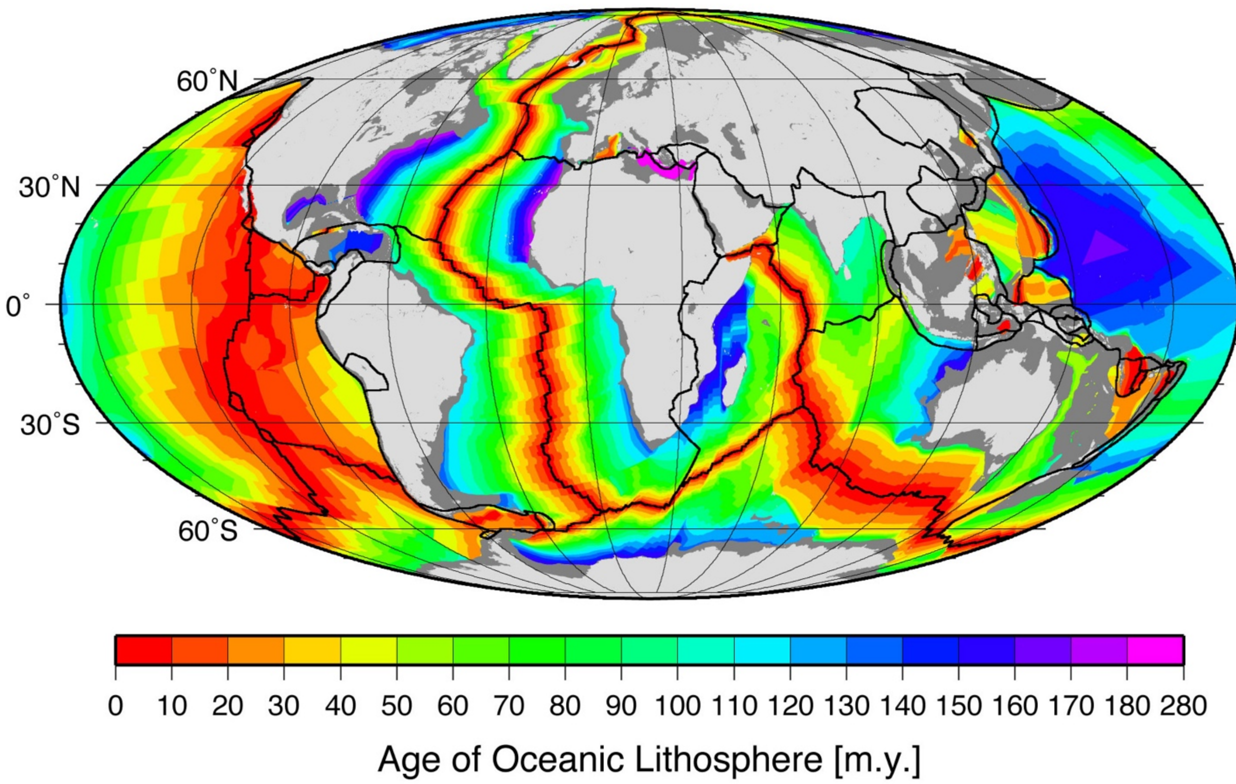

Figure 1. Map showing the age of the seafloor and locations of mid-ocean ridges. Relative widths of the 0-10 million year (m.y.) age seafloor (in red) reflects the variation in spreading rate on different mid-ocean ridges. For example, the southern East Pacific Rise spreads at up to 15 cm/yr, whereas the northern Mid-Atlantic Ridge spreads at only 2-3 cm/yr.

Understanding MOR volcanism is important because eruptions and hydrothermal activity represent major transfers of heat and chemical compounds from the solid earth to the oceans and are therefore key to understanding the global energy and chemical budgets of our planet. MOR hydrothermal systems also host extensive and unique ecosystems (SDG 14) on the seafloor and form massive sulfide ore deposits in the subsurface (SDG 7,12). This is because circulating geothermal fluids can attain higher temperatures without boiling under the high pressure of the deep ocean, allowing them to efficiently leach and mobilize valuable elements out of the surrounding rocks. This ore formation process, studied in modern MOR hydrothermal systems where those processes are active today, has transformed our concepts about ore-forming systems and provides insights into ancient ore deposits now exposed in fragments of oceanic crust called ophiolites that have been thrust up on land. With international interest in seabed mining of ore deposits on the rise, there is urgency to identify environmental impacts and ecosystem-based management practices for deep ocean environments (SDG 7, 12, 14).

Mid-ocean ridge volcanism occurs in a narrow zone ~5-30 km across where Earth's tectonic plates are moving apart. This divergent motion causes the underlying asthenospheric mantle to well up under spreading centers, leading to decompression melting that supplies magma to crustal reservoirs, which in turn feed intermittent effusive eruptions on the seafloor and form thick layers of coarse-grained gabbroic rocks in the subsurface. Partial melting of the mantle mainly produces basaltic lavas that are erupted from fissures and fed by dikes. However, the character and frequency of MOR volcanic activity and the physical landforms it produces on the seafloor vary greatly as a function of spreading rate and magma supply. The amount of magma, and therefore heat, delivered to the crust per unit time in a particular location strongly affects the temperature profile beneath the axis, with important consequences for magma storage and evolution, its availability for crustal construction, and ultimately the frequency, style, and dynamics of seafloor volcanism.

Since plate spreading rate is a primary driver of decompression melting, ridges with fast spreading rates are expected to have higher average magma supply (the flux of magma per unit time) than ones with slow spreading. This is supported by the fact that the average thickness of the oceanic crust is ~6 km over most of the spreading rate range [2], suggesting a linear increase of the magma flux with spreading rate. Many fundamental characteristics of ridges have been shown to vary with spreading rate, including ridge morphology, segmentation, composition, and accretion style. In some locations however, magma supply is decoupled from spreading rate due to thermal or compositional anomalies in the mantle (e.g., spreading centers near hotspots or in back-arc settings), and numerous studies in recent decades have shown that magma supply is a key parameter driving many of the primary features of MORs [3]. Variations in magma supply generate a continuum in how plate spreading is accommodated, from mainly by magmatic processes (via dike intrusion and eruption) at the fast-spreading, magma-rich end of the spectrum, to mainly by tectonic processes (via normal faulting) at the slow-spreading, magma-poor end of the spectrum. Different parts of this spectrum produce very different ridge crest morphology and patterns of ridge segmentation on the seafloor. In general, there is more variability in MOR volcanism and tectonism at the slow- and ultra-slow spreading end of the spectrum, where magma supply can be highly variable in space and time.

The highest MOR spreading rates on the planet (>15 cm/yr) are found along the southern East Pacific Rise (EPR) west of Chile, whereas the slowest spreading rates (<2 cm/yr) are found along the Arctic ridges north of Iceland, at the Red Sea rift, on the Mid-Cayman Rise, and on the Southwest Indian Ridge south of Africa. The effect of variable MOR spreading rates can be seen on a global map of seafloor age, with faster-spreading ridges creating more seafloor in a given amount of time (Fig. 1). Another way to illustrate the range of spreading rates is the simple calculation that to create space for a 1-m wide dike, it would take 5-10 years of spreading on the southern EPR, but 50-100 years on the Arctic ridges. Spreading events are fundamentally intermittent and cyclic, with the frequency of eruptions depending on spreading rate and magma supply.

In stark contrast to the situation above sea-level where volcanic eruptions are easily observed and can have profound impacts on human lives, no deep-sea MOR eruptions have ever been directly witnessed (although a few eruptions in submarine volcanic arcs have been filmed [1]. On the other hand, since 1991 at least 20 historical eruptions on the submarine parts of the global MOR system (not counting Iceland) have been documented in one of the following ways: (1) a combination of luck, good timing, and repeated time-series observations, (2) searching for hydrothermal plumes of unusual size and chemistry in the water column, (3) depth changes revealed by repeated bathymetric mapping produced by new lava flows [4], (4) remote detection using hydrophones, or (5) focused observatories with instrumental monitoring networks on the seafloor in a few locations. Nevertheless, many MOR eruptions that are undetected must occur each year.

This overview and description of MOR volcanism is an update on previous review papers [5]. Many of the concepts described below also apply to back-arc spreading centers, where similar volcanic processes occur but in a different tectonic environment.

2. Mid-Ocean Ridge Eruptions

Because of their dominantly extensional setting, MOR eruptions are the underwater equivalent of dike-fed “curtain-of-fire” eruptions in volcanic rift zones on land. However, the resulting eruptive products can be quite different in the submarine environment due to the confining pressure of the overlying water column, which restricts the exsolution of magmatic gasses, and the enhanced cooling effect of frigid seawater compared to air, which leads to more rapid formation and thickening of glassy crusts on submarine lava during its emplacement. Interpreting lava emplacement processes in the deep ocean requires multiple scales of observation. For years, studies of MOR morphology were limited to either observing at the coarse scale of ship-based multibeam sonar bathymetry (resolving features 10s to 100s of meters across) or at the fine scale of visual observations from submersibles or deep-towed cameras (resolving features up to several meters across), with a large observational gap in between that made it difficult to relate one to the other. More recently, that gap has been filled by high-resolution bathymetry from autonomous underwater vehicles (AUVs) that can map the seafloor at 1-m resolution. This significant advancement allows for much more effective geologic mapping of volcanic terrain on the seafloor and can be used to place “photo-scale” visual observations (Fig. 2) in the more meaningful context of “map-scale” volcanic morphology (Fig. 3). This has enabled geologic mapping of some MOR volcanic systems in great detail [6], especially when combined with lava geochemistry and innovative dating methods [7].

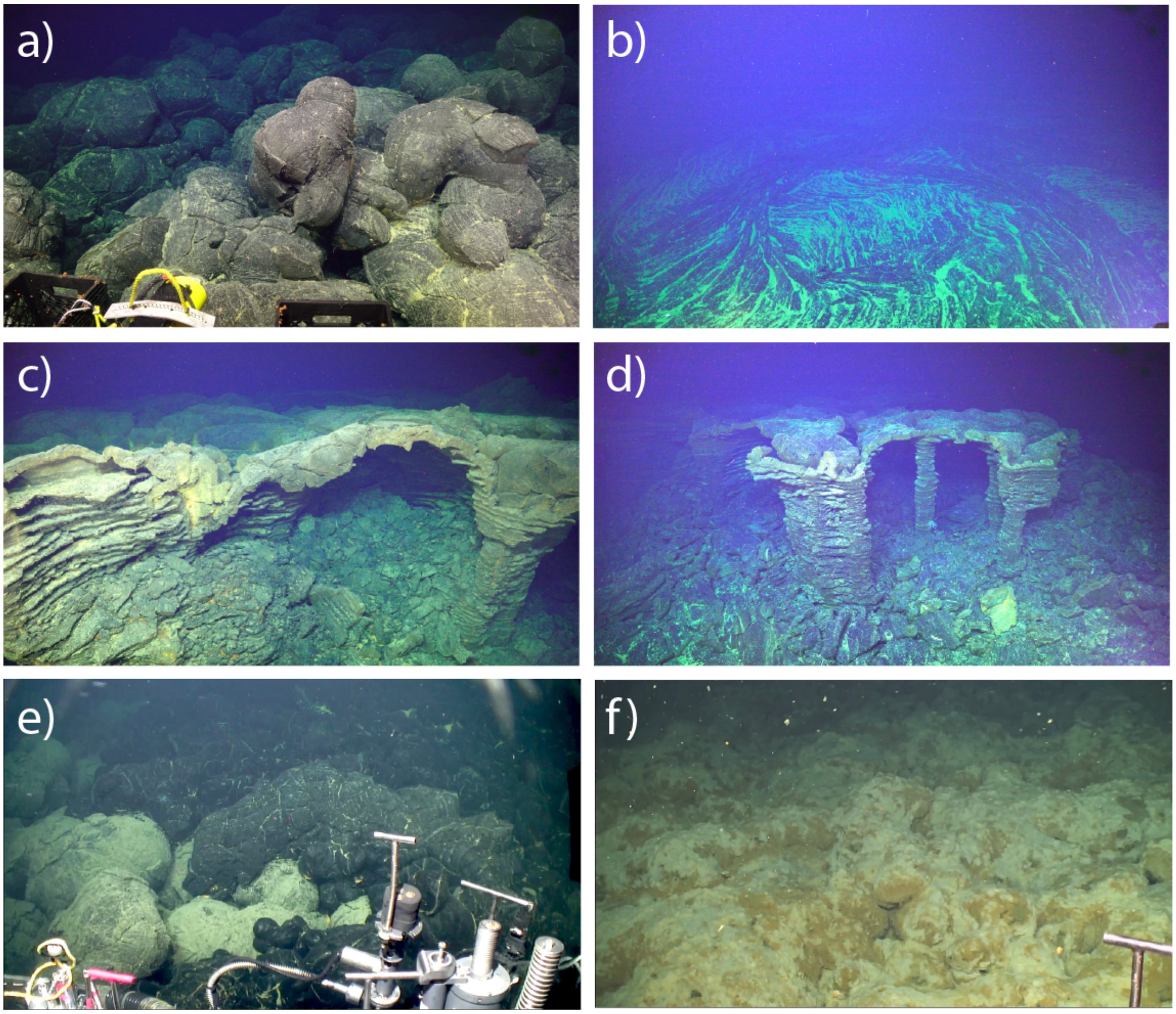

Figure 2. Photos showing the range of submarine lava morphologies; all are video framegrabs from ROV *Jason* dives at Axial Seamount. (a) Pillow lava. (b) Ropy to lineated sheet flow. (c) Collapse area in a lobate sheet flow where the molten interior has drained out below a solid crust. (d) Lava pillars exposed within a collapse area of a lobate sheet flow. (e) Contact between 2015 lava (dark, glassy, upper right) over older seafloor (lighter sedimented pillows, lower left). Photo taken 4 months after the eruption at the thin flow margin where no “eruption mat” formed. (f) Thick “eruption mat” covering a 13-m thick pillow lava flow, only 4 months after it erupted in 2015. The mat is formed by microbial growth where thick lava flows vent warm hydrothermal fluids as they cool. The mat disappears after a few years after the flows have cooled.

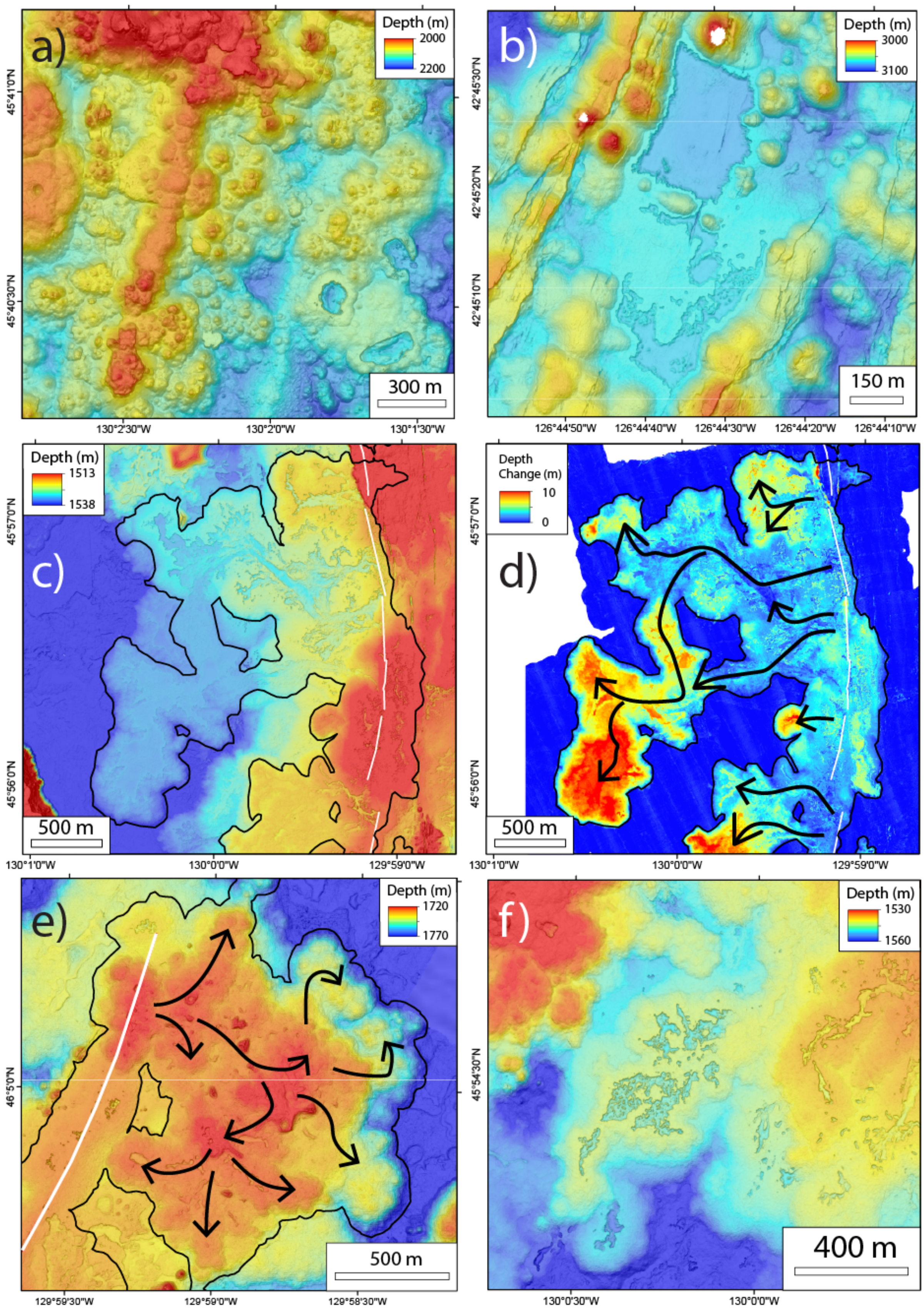
a)
Depth (m)
2000
2200
300 m
45°41'0"N
45°40'30"N
130°2'30"W
130°2'0"W
130°1'30"W
b)
Depth (m)
3000
3100
150 m
42°45'30"N
42°45'20"N
42°45'10"N
126°44'50"W
126°44'40"W
126°44'30"W
126°44'20"W
126°44'10"W
c)
Depth (m)
1513
1538
500 m
45°57'0"N
45°56'0"N
130°1'0"W
130°0'0"W
129°59'0"W
d)
Depth
Change (m)
10
0
500 m
45°57'0"N
45°56'0"N
130°1'0"W
130°0'0"W
129°59'0"W
e)
Depth (m)
1720
1770
500 m
46°5'0"N
129°59'30"W
129°59'0"W
129°58'30"W
f)
Depth (m)
1530
1560
400 m
45°54'30"N
130°0'30"W
130°0'0"W

Figure 3. Map-scale observations of the seafloor from 1-m-resolution bathymetry collected by AUV. (a) South rift zone of Axial Seamount showing morphology of pillow mounds and ridges. (b) Northern Gorda Ridge showing contrasting volcanic morphology of high-standing pillow mounds (in yellow and red, above 3050 m depth) and ponded sheet flows with areas of collapse filling low-lying areas (in light to medium blue, below 3050 m depth). (c) Bathymetry and (d) depth changes before/after the 2011 eruption at Axial Seamount showing channelized sheet flows (black outlines) on gentle slopes near the eruptive vents (white lines) and thicker inflated lobate lava lobes at distal flow fronts. (e) A 60-m thick lobe of 2015 lava (black outline) erupted from fissures (white lines) on the north rift zone of Axial Seamount. Lobe has pillows on the steep sides, and lobate lava on the top with tumuli and collapse areas. (f) Large flow lobe with pillowed margins and lobate top with extensive dendritic collapse areas in the interior of the lobe, south of the caldera at Axial Seamount.

Laboratory analog experiments have shown that the range of morphologies on submarine lava flows primarily reflects eruption rate, which affects how the solidifying surface crust interacts with the molten interior of a flow during its emplacement, which in turn is reflected in the landforms that they create on the seafloor. During slower effusion, individual pillow lava lobes form a crust on all sides (Fig. 2a) and tend to pile up to construct thick, steep-sided, haystack-shaped hummocky mounds or ridges (Fig. 3a) that can be over 100 m thick, up to a few 100 m wide, and up to a few km long [8]. Pillow mound eruptions can occur over periods of days to weeks. In contrast, at higher effusion rates, sheet flows form as individual lava lobes quickly coalesce and spread out into a thin broad sheet with a crust on the top and bottom and an interior that remains molten for a short time (Fig. 2b). Because of this, sheet flows tend to fill in low areas in the landscape, commonly ponding in closed basins or becoming channelized on slopes (Fig. 3b). Single flows can have thin lobate sheet morphology near eruptive vents, can become channelized downslope, and can form inflated, pillowed flow lobes at their distal ends (Fig. 3c, d) [6]. Once they stop spreading laterally, ponded sheet flows often inflate upward if the lava keeps being fed to the molten interior, which can lift the flat upper crust by 5-10 m or more. Sheet flow emplacement can be rapid and short-lived (minutes to hours), and they often contain extensive areas of collapse (Fig. 2c) where the molten flow interior has either drained back into the eruptive fissures or drained out downslope and the original upper crust has foundered where it was left unsupported (Fig. 3b). Lava pillars are features unique to the submarine environment that are often found within the collapsed interiors of lobate sheet flows (Fig. 2d) and preserve evidence of the flow inflation and drain-out process.

Submarine lava morphology is also strongly influenced by local slope and bathymetry, and single lava flows can have a wide range of morphologies due to the local variation in emplacement rates, slopes, and the sequence of events during emplacement (Fig. 3e, f). Similarly, the earliest flows during a single eruption can be emplaced as thin sheet flows when eruption rates are higher, and later parts of the eruption can produce thick pillow mounds after eruption rates decline [4].

The proportion of pillow flows to sheet flows at MORs is often correlated to the spreading rate, however more recent work suggests that magma supply likely exerts the primary control. Fast-spreading MORs, with their overall high magma supply, have a high proportion of sheet flows, and pillow mounds are rare on-axis and somewhat more common off-axis. In contrast, eruptions at intermediate- and slow-spreading ridges, where magma supply is much lower and more variable, display a larger range of morphologies. While hummocky mounds and ridges are typical of the neovolcanic zone at slow-spreading ridges [8], periods of increased magma supply can locally produce a higher proportion of sheet flows similar to what is observed on faster spreading MORs. These differences in eruption style lead to differences in the gross morphology of the neovolcanic zone at different spreading rates.

Fragmental products from degassing and/or explosive activity have been documented in deep-sea MOR environments, but these deposits are generally only a minor component of most eruptions. Bubble wall shards and limu o Pele have been found at some deep MORs and have been attributed to explosive magmatic degassing, or CO_2-rich eruption onsets with low-energy strombolian activity. This style of activity has not been witnessed, but volcaniclastic deposits have been produced at several historical MOR eruption sites, suggesting it is not uncommon. Other volcaniclastic deposits with distinctive lithofacies have been attributed to less common phreatomagmatic activity associated with caldera collapse events when seawater is suddenly exposed to hot rock in subseafloor hydrothermal systems.

3. Ridge-Axis Morphology and Segmentation

At broader scales (kms to 100s of kms), the morphology of MOR plate boundaries is determined by the relative interplay between volcanic construction and tectonic dismemberment, processes which are highly variable and dependent on spreading rate and magma supply [9]. MOR morphologies range from axial highs typical of fast-spreading ridges to deep, wide and sometimes asymmetric axial valleys generally associated with slow- and ultraslow-spreading ridges (Fig. 4a). Intermediate-rate spreading centers may have an axial high or an axial valley, depending on the magma supply.

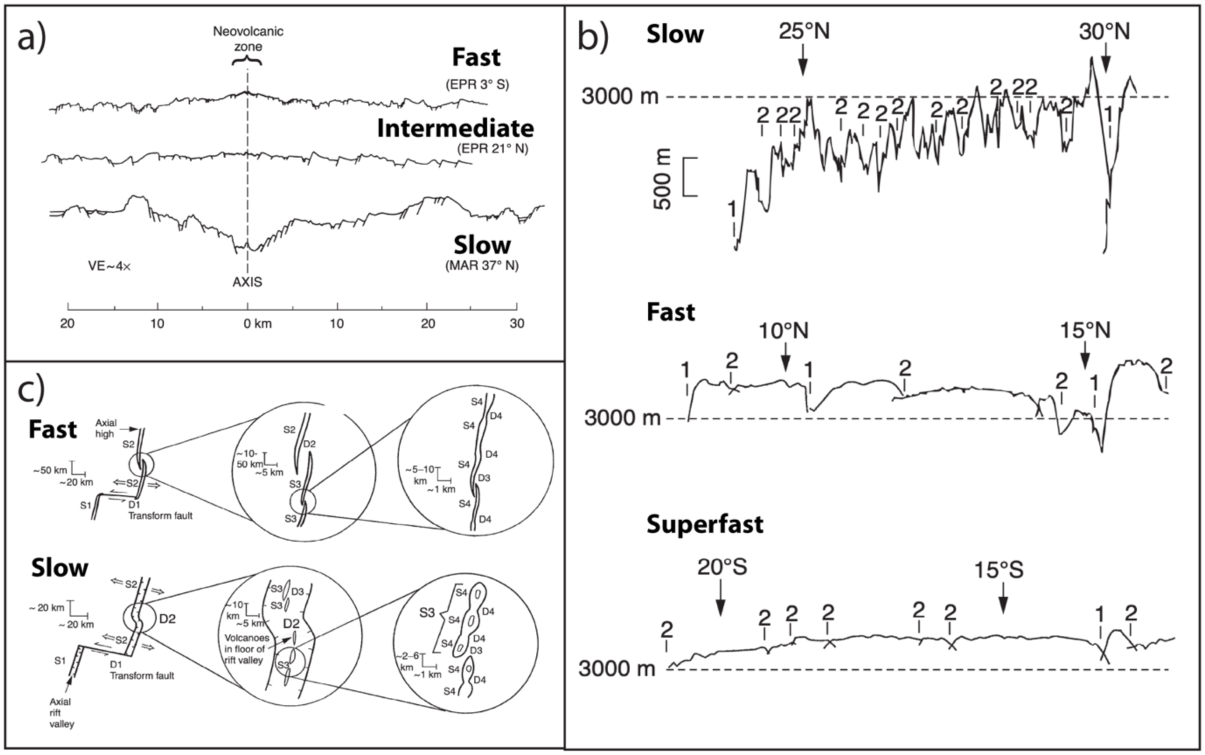

Figure 4. Variations in ridge crest morphology and segmentation versus spreading rate. (a) Cross-axis depth profiles comparing ridge axis morphology at fast, intermediate, and slow spreading rates. (b) Along-axis depth profiles comparing slow, fast, and superfast spreading ridges. (c) Comparison of ridge segmentation style at fast and slow spreading rate ridges.

Axial highs develop above regions of high magma supply from constructional volcanism and the buoyancy of low-density and partially molten material that resides at shallow depths (typically less than 3 km) beneath the ridge axis. In this setting, plate spreading is largely accommodated by dike intrusion, some of which breach the surface and erupt lava on the seafloor, and normal faulting is secondary. In other words, as plate divergence accumulates extensional stress across the plate boundary, magma is usually available beneath the ridge crest with a high enough driving pressure to intrude dikes to relieve those extensional stresses. Over time, this creates a high axial morphology characterized by a ridge crest that is continuous and gently undulating along-strike, and deepens to either side across-strike (Fig. 4). The ridge crest is commonly bisected by a narrow axial summit trough, 10-100 m wide and deep, interpreted as the result of near-surface faulting above dikes intruded within a narrow neovolcanic zone [10].

In contrast, in regions of lower melt supply (at slower spreading ridges), the thickness of cooled and rigid rocks on-axis (the axial lithosphere) is greater, and magma is not always available to feed crustal dikes, leaving more of the extension to be accommodated by normal faulting. Consequently, the morphology of low-magma-supply MORs is characterized by large fault-bounded axial valleys that are generally 10-30 km wide and 1-2 km deep. Along some magma-poor sections of slow-spreading MORs, faulting is so prevalent that large offset normal faults develop (also called detachment faults), leading to the exhumation of mantle rocks, formation of oceanic core complexes, and an asymmetric axial valley. Within an axial valley, the shallowest and narrowest part of the seafloor is often near the segment center, and volcanism along the valley commonly forms constructs called axial volcanic ridges. These volcanic ridges are composite constructs of multiple eruptions over 100s or 1000s of years, with the basic building blocks being pillow mounds, ridges, and "hummocks" [8].

These differences in ridge morphology are well-illustrated in both cross-axis and along-axis depth profiles of fast, magma-rich and slow, magma poor ridges (Fig. 4a, b). The wavelength of undulations in axis depth at fast-spreading ridges is 10s of km and with an amplitude of 10s to 100s of meters. In contrast, at slow-spreading ridges the wavelength is much shorter and the amplitude much larger. These variations in axial depth are generally interpreted as reflecting the relative magma supply along ridge segments, with higher supply along shallow portions of ridges and lower supply at the deeper segment ends. At slow-spreading ridges, magma bodies are thought to be smaller, more isolated, and shorter-lived than at fast-spreading ridges [9, 11].

Discontinuities of the MOR ridge axis along strike occur at a range of scales that have been described in a hierarchy of segmentation (Fig. 4c), from 1st-order (transform faults with offsets of > 100km with a longevity of up to 100s of Ma) to 4th-order (offsets of < 1 km with a longevity of < 10-100 yrs) [12]. First- to third-order discontinuities usually form depth maxima on axial depth profiles, and are sometimes associated with changes in chemical composition that suggest correlating changes in magma distribution along strike. Seismic imaging shows corresponding discontinuities of the axial magma lens at fast- and intermediate-spreading ridges. On a fundamental level, these different scales of segmentation partially define what constitutes a "volcano" at MORs (a term that can be otherwise difficult to apply to continuous, linear volcanic systems), and second- and third- order ridge segments can be considered individual volcanic systems with their own separate magma supplies.

---

4. CASE STUDY BOX: Insights From Historical Eruptions

Some things can only be learned by catching eruptions in the act, but this is much more challenging in the deep ocean than on land. Nevertheless, historical MOR eruptions that have been well-documented have provided quantum leaps in our understanding of active processes. Here, we highlight some of the insights gained from two sites with well-documented eruptions (Fig. 5): Axial Seamount, a hotspot volcano on the intermediate-spreading (6-cm/yr) Juan de Fuca Ridge (JdFR) in the NE Pacific, and the 9°50'N segment of the fast-spreading (11 cm/yr) East Pacific Rise (EPR). Both of these sites have had multiple eruptions in the last 30 years (1998, 2011, and 2015 at Axial, and 1991-2 and 2005-6 at the EPR at 9°50'N). The two sites have significant morphological differences. Axial is a ~1000-m-high seamount (summit depth ~1400 m) with a 3 x 8 km caldera and two rift zones that extend for ~50 km north and south, forming the most magmatically robust segment of the JdFR. In contrast, the EPR at 9°50'N is the apex of a 3rd-order ridge segment (extending from 9°-10°N) whose depth varies gently along the spreading axis (2510-2580 m) [10].

Documented historical eruptions provide rare clarity on the extent, thickness, and volume of individual eruptions because the unsedimented glassy appearance of new lava flows is easily distinguished from older lavas with sediment cover (Fig. 2e), and in some cases before-and-after bathymetry can quantitatively constrain depth changes on the seafloor [4, 6]. This enables geologic mapping of lava morphologies relative to eruptive fissures, identification of channel systems that distribute lava away from the vents, and interpretation of the sequence of events during lava emplacement. However, a unique aspect of submarine eruptions is that where new lava flows are thick (>10 m) and/or near the eruptive vents they can become covered by microbial mats that grow while the flows cool, and can completely mask the fresh glassy appearance of the lavas (Fig. 2f).

The 2005-2006 eruption on the EPR at 9°50'N (Fig. 5a) occurred along 17-18 km of the ridge crest, but at variable effusion rates along strike, and lava flowed up to 3 km away from the axis [6]. This eruption occurred in about the same area as the 1991-1992 eruption but was 4-5 times larger in volume. The 2005-2006 eruption mainly produced inflated lobate sheet flows with an average thickness of 1-2 m, with pillows at the distal flow fronts, locally up to 5-10 m thick [6]. The 4th-order ridge segmentation mapped at the seafloor appears to reflect discontinuities in the underlying axial magma lens that has been seismically imaged at a depth of 1.4-1.6 km.

Just like at volcano observatories on land, long-term seismic and geodetic monitoring of submarine volcanoes have greatly increased our understanding of active processes during multi-year eruption cycles as well as during individual eruptions. At the EPR at 9°50'N, the seismicity before and during the 2005-2006 eruption was recorded by a temporary network of ocean-bottom seismometers. Long-term measurements of hydrothermal vent temperatures used to calculate crustal permeability show evidence of a cycle that suggests causal linkages between magmatic and hydrothermal activity that could be useful for forecasting future eruptions.

At Axial Seamount (Fig. 5b), a multi-decadal record of vertical deformation in the summit caldera shows a pattern of rapid co-eruption deflation separated by longer periods of gradual inter-eruption inflation, and the pattern has been repeatable enough that it was used to successfully forecast the 2015 eruption. This record shows that the magma supply at Axial has been continuous since at least 1998, but at a rate that has varied with time by over an order of magnitude. Between eruptions, magma is stored in a large reservoir beneath the summit caldera, and during eruptions magma is intruded into dikes that initially erupt sheet flows in the summit caldera and then propagate laterally 10's of km into one of the two rift zones where large pillow mounds are extruded and emplaced [4]. At Axial, most of the volume of the historical eruptions have been emplaced in these pillow mounds (up to 140-m thick) at the distal ends of dike intrusions [4].

At Axial, seismicity is initially low for several years right after an eruption and then increases exponentially as a function of cumulative inflation as the roof of the magma reservoir is increasingly stressed. The seismicity at Axial mainly occurs on outward-dipping caldera faults above the magma reservoir and has been shown to be highly sensitive to the ocean tidal cycle. At both Axial and the EPR at 9°50'N, some eruptions have produced impulsive sounds during lava emplacement (likely from lava-water interaction, possibly due to implosions of drained lava lobes) that were recorded by local seismic networks, helping to clarify eruption extent, duration and the timing of lava emplacement [4, 6]. The volumes of the historical eruptions at the EPR at 9°50'N have ranged from 4-22 x 10^6 m^3 [6], and from 24-155 x 10^6 m^3 at Axial [4].

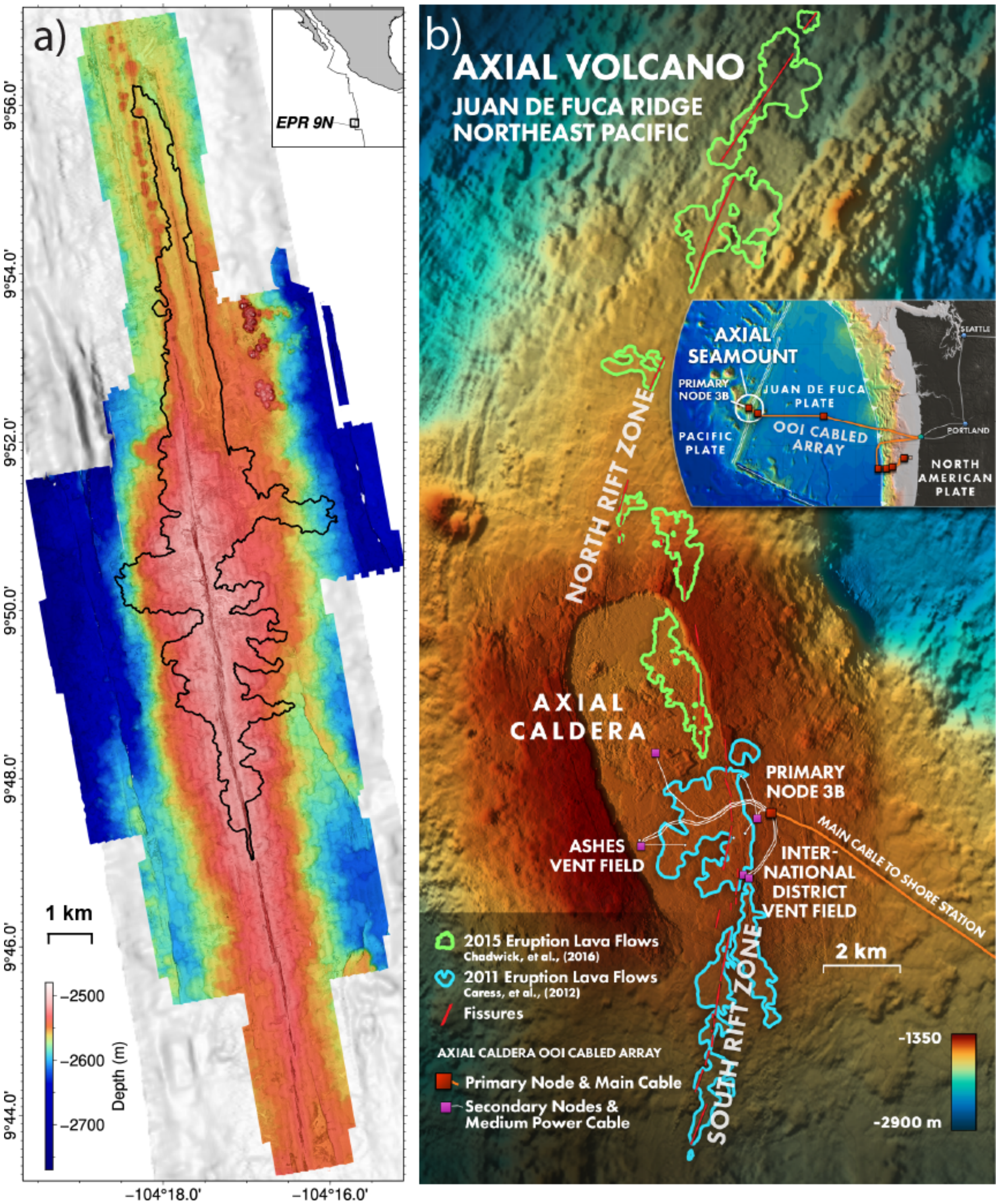

Figure 5. Examples of historical MOR eruptions. (a) Map of new lava erupted in the 2005-2006 eruption on the East Pacific Rise at 9°50'N, outlined in black. (b) Map of Axial Seamount, Juan de Fuca Ridge, showing outlines of lava flows from the 2011 and 2015 eruptions.

---

5. Magma Supply and Storage

As at other volcanic systems, MOR eruptions are fed by magma stored in the crust and/or the uppermost mantle. Most of this magma never erupts, with an estimated 75-80%

cooling and solidifying into gabbroic intrusive bodies. What does reach the surface shows signs of at least some cooling and differentiation (e.g., olivine and plagioclase crystallization) prior to eruption. Sorting out how and where this magma is stored, and the nature and timescales of processes within these storage areas, are areas of active research and debate. One consistent finding from seismic experiments and petrological studies is that many key features of MOR magma plumbing systems vary with overall magma supply and spreading rate (Fig. 6).

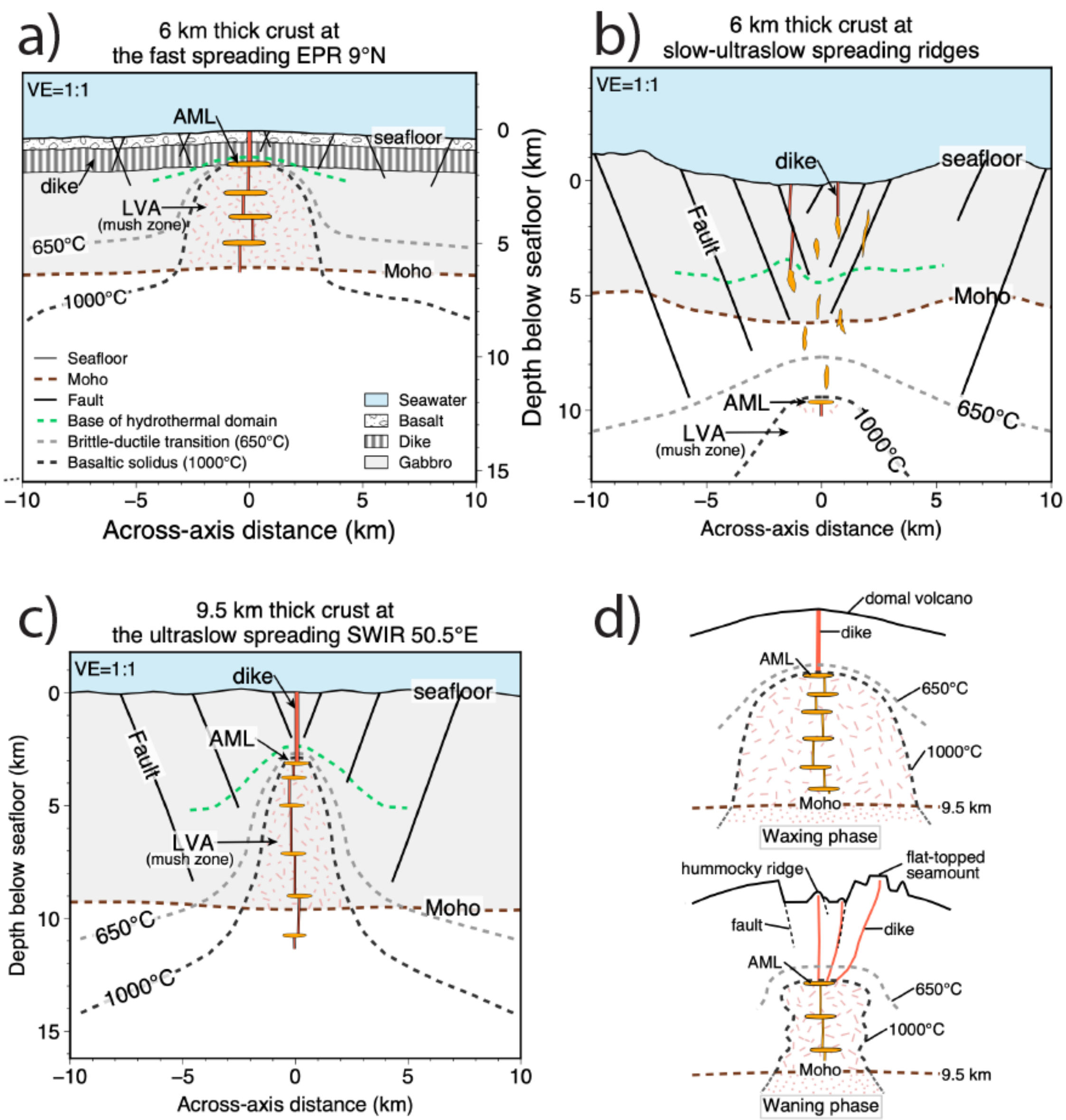

Figure 6. Schematic cross-sections showing the thermal consequences of variable magma supply beneath mid-ocean ridges at different spreading rates (AML = axial melt lens, LVA = low-velocity anomaly). (a) Cross-section of the 6-km thick crust at the fast-spreading East Pacific Rise (EPR) at 9°50'N with a higher magma supply. (b) Cross-section of the 6-km thick crust at a slow-ultraslow spreading segment of the Southwest Indian Ridge (SWIR) with a lower magma supply. However, slow-ultraslow spreading ridges can also undergo periods of higher

magmatism, shown by the cross-section in (c) of the magmatically robust but ultra-slow spreading SWIR 50.5°E segment with a 9.5 km-thick crust and a crustal LVA. These differences at the ultraslow-spreading end of the spectrum can be explained by the thermal effects of cyclic changes in melt input, shown by (d) comparing the waxing (top) and waning (bottom) phases of a fluctuating magma supply.

At high magma supply, fast-spreading ridges, seismic reflection experiments have consistently imaged the roof of a shallow and thin (< 100 m) axial melt lens located 1 to 3 km below the seafloor and extending 2-4 km across axis (Fig. 6a). The compositions of lavas that erupt at these ridges are consistent with this, with major element trends indicating the magmas cool and partially crystallize at relatively low pressures (< a few kb) in the shallow crust prior to eruption. The strength of this melt lens reflector varies along-axis, probably reflecting varying proportions of melt and crystals. These magma storage areas must be replenished relatively frequently to sustain a significant portion of melt without it freezing in the otherwise cool, shallow crust. Variations in supply can also lead to upward and downward migration of the magma lens, as suggested by ophiolite studies and drilling results [13]. The resulting lavas show limited variability in various trace element and isotope ratios that suggest the incoming mantle melts are being mixed and homogenized in these crustal storage areas [14]. This combination of mixing and chemical differentiation tends to obscure deeper processes and more primary melt compositions. Although the vast majority of sampled MOR lavas are basalts, more evolved compositions (e.g., andesites and dacites) can also be found, indicating a broader range of temperature conditions and crystallization extents can also occur locally.

While this shallow melt lens may be the most obvious expression of magma beneath fast-spreading ridges, recent studies show evidence for a more complex magma plumbing system, with some crystallization occurring at greater depths. As olivines crystallize, they sometimes capture the surrounding liquid, forming melt inclusions whose compositions indicate that crystallization occurs in the lower crust or upper mantle [15]. Similarly, seismic imaging shows the shallow melt lens tops a broader domain at least 4 to 5 km thick with low seismic velocities interpreted as a crystal-dominated mush (Fig. 6a). More recent seismic experiments have shown that this crystal-dominated mush domain also hosts deeper melt-dominated lenses [16]. The geometry and strength of the associated reflectors changed following the 2005-2006 eruptions at EPR 9°50'N, suggesting that melt in these deeper lenses was transferred to the shallow melt lens, from where it then erupted.

As magma supply decreases at slower-spreading ridges, subaxial storage areas deepen and become less continuous (Fig. 6b). Unlike fast-spreading ridges, slow and ultraslow ridges mostly lack a melt lens seismic reflection despite evidence of widespread eruptive activity. Due to their relatively low magma supply, it is likely too cold in the shallow crust to sustain a melt-rich reservoir for long, so the chance of detecting one during a given seismic experiment is low. However, seismic refraction experiments along slow spreading ridge segments have found areas deeper in the crust with significantly lower seismic velocities indicating high temperatures and, in some cases, small amounts of melt [17]. These crustal magma reservoirs top out at depths between 2.5 and 4 km below the seafloor, and extend just a few kilometers along-axis at the center of magma-rich ridge segments, where the crust is anomalously thick (Fig. 6c). Longer lasting melt reservoirs (in the form of melt lenses or melt-rich crystal mush) may only reside at greater depth in these settings, but such deep melt-rich reservoirs remain hypothetical at this point, being beyond the depth range of most current MOR seismic experiments.

As the seismic melt lens deepens and eventually disappears, corresponding compositional changes in the erupted lavas also point to changes in their magmatic history. Lavas erupted from slower spreading (low magma supply) ridges tend to be less differentiated and less well-mixed on average [14]. They also show evidence for higher crystallization pressures on average, consistent with deeper magma storage. This change in magma storage is key to understanding the seeming paradox that cooler, lower supply MORs erupt hotter, less evolved magmas: they likely erupt from deeper in the crust, where ambient temperatures are higher.

Magma supply is both spatially and temporally variable at slow spreading rates, with some areas of slow MORs exhibiting an exceptionally thin and discontinuous volcanic layer. Observations from gabbros and ultramafic rocks exposed by faults at or near the surface in these locations suggest significant amounts of magma may get trapped in the mantle. These and similar locations offer rare and useful glimpses into the lower crust and upper mantle, where processes are poorly understood. Many gabbros and abyssal peridotites show evidence of reactive porous flow and mineral dissolution during melt migration, suggesting that melt-rock reactions are common in the lower crust and upper mantle [18, 19].

The handful of observations of shallow melt reservoirs at slow and ultraslow segment centers likely represent current episodes of greatly enhanced magma influx (Fig. 6d) [3]. The durations and frequencies of these magma flux variations are poorly constrained. A relatively long duration (~ 300 kyrs) is estimated from the study of volcanic morphologies at these magma-rich, slow-ultraslow ridge segment centers. Shorter durations (~ 10 kyrs or less) during which melt flux would be enhanced by an order of magnitude or more are also possible, based on estimates of hydrothermal heat fluxes of black smoker systems at slow spreading ridges. These hydrothermal constraints also apply to fast spreading ridges, where active black smoker systems are now understood to be evidence of episodes of enhanced magma input to the ridge axis [16].

6. Mantle Melting Processes

For MOR lavas, eruption at the seafloor marks the finish line of a long journey that starts with partial melting of the mantle deep beneath the ridge, and involves partial crystallization, mixing, and complex melt-crystal and melt-rock interactions in the mush domains, magma bodies, and dikes that form the ridge's magma plumbing system. The geochemistry of MOR lavas bears witness to all of these processes, yet it remains a challenge to decipher their respective effects and determine basic parameters such as the composition of the melting mantle, and how melts migrate upwards through the melting regime and eventually accumulate beneath the ridge axis.

Plate divergence leads to upward flow of the asthenospheric mantle, which eventually crosses its solidus, triggering the onset of partial melting. The depth at which this occurs depends on mantle composition and on mantle temperature: a mantle enriched in incompatible elements (for example Al, Na, K) has a deeper solidus than a mantle depleted in these elements; and for a given composition, a hotter mantle crosses its solidus at a greater depth.

For the range of estimated MOR mantle compositions and temperatures, solidus depths for dry mantle away from hotspot regions are estimated to range between 40 and 100 km [20], likely with small extents of partial melting occurring even deeper due to small amounts of water in the mantle.

The amount of melt supplied to the ridge is a function of the mantle's upward velocity, as well as the shape and size of the region from which melts are efficiently extracted and focused to the ridge. MOR melts are fluid and less dense than their parent mantle and therefore buoyant, rising independently and significantly faster than the upwelling solid mantle. The extent to which melts are effectively extracted from the mantle, and the degree to which they react with their surroundings during melt migration and subsequent storage, have significant predictable consequences for melt fluxes and on MOR magma composition. With no access to pristine samples of the mantle source or its primary melts, and given that available geophysical methods (seismology, electro-magnetism) are too low in resolution at such depths to image melt channels or other plumbing features, numerous aspects of the melt regime remain poorly understood. However, extensive modeling efforts combined with recent observations provide some useful constraints. Current estimates of melt migration rates are on the order of 10s of meters per year, too fast to be explained by diffuse porous flow alone [21]. Such rapid transport rates are consistent with most melt being concentrated into high-permeability channels, which various models predict to arise from some combination of processes such as reactive flow instability, compositional heterogeneity, and decompaction weakening. These permeable channels eventually converge towards the ridge axis, although the exact mechanisms responsible for focusing melts from such a broad melting regime (~100s of km wide) to such a narrow region of crustal accretion (~a few km) at the axis are debated. A ~1-km-long section of mantle recently recovered by ocean drilling shows abundant evidence for small (cm-scale) channels of reactive flow and oblique melt transport [19].

Although crustal magmatic processes modify the geochemical composition of incoming melts, certain trace elements and isotopes help provide useful insights into melting processes and the mantle source composition. In recent decades, high-resolution geochemical analyses conducted on melt inclusions and cumulate materials have found that the melts coming out of the mantle are compositionally heterogeneous [14]. The degree to which these compositional variations are generated during the melting process as opposed to inherited from the mantle source is unclear, but fractional melting and disequilibrium melt transport processes are likely needed to preserve this heterogeneity. Much of this geochemical diversity seems to be lost during subsequent mixing and fractional crystallization, although studies differ on where exactly this mixing occurs. Recent geochemical compilations of MOR lavas also suggest that the mantle source is less depleted on average than previously assumed, with a range of depleted and enriched compositions commonly occurring at normal ridge segments (far from enriched hotspots).

Another key observation regarding MOR mantle melting processes and the resulting melt fluxes comes from studying the thickness and configuration of the oceanic crust it produces. While low supply regions of slow-ultraslow spreading ridges include a significant component of serpentinized mantle-derived peridotites in their crustal layer, overall the oceanic crust is overwhelmingly formed of rocks that crystallized from MOR magmas (gabbros, dolerites and basalt). Therefore, looking at a regional scale that integrates several ridge segments, the thickness of the oceanic crust is a measure of the time-integrated MOR melt flux. It is remarkable that, if one ignores ridges near hotspots, the average oceanic crust is ~6 km thick for all but the lowest spreading rates [2]. This first order observation suggests that mantle upwelling is largely passive—it is primarily driven by and compensates for plate divergence. At smaller scales, however, geodynamic models indicate that the buoyancy of low-density, partially molten mantle likely drives additional mantle upwelling. These density effects are expected to be more pronounced at slow spreading rates, where they may help explain the larger amplitude variations in crustal thickness observed there. In addition, another non-mutually exclusive hypothesis suggests that melt migrates towards the center of slow-spreading ridge segments along the permeable and sloping base of the axial lithosphere. These combined magma focusing effects likely help explain the along-axis variability in crustal construction along slow-spreading ridges.

7. Summary

The majority of Earth's volcanism occurs along mid-ocean ridges in the deep ocean, but is usually undetected and unseen, which limits our understanding of this fundamental planetary process. However, recent research and advances in technology continue to contribute to our growing knowledge base. Modern seafloor observatories at a few sites now enable us to detect and monitor seafloor eruptions as they are happening, a critical window into active processes. High-resolution mapping of the seafloor can be used to interpret submarine lava emplacement, and when combined with geochemistry and innovative age dating, can reveal the recent eruptive history at individual volcanic systems. Seismic imaging of subsurface magma bodies in the crust below MORs gives constraints on the depth and spatial extent of melt in the subsurface, and repeated surveys show changes over time. Geochemical fingerprinting of crustal materials combined with sophisticated modeling provides clues about the deeper processes in the mantle that generate melts and transport them upwards into crustal storage zones to eventually feed eruptions at the seafloor. The rich variety in the characteristics of MOR volcanism in different tectonic settings can be understood as a consequence of how magma supply and plate spreading rate vary in space and time.

Insert **QR code #2** here for online Appendix with **References for Further Reading – one list with all references**

Insert **QR code #3** here for online Appendix with **References for Further Reading – six lists, organized by Chapter Section**

Insert **QR code #4** here for online Appendix with **Information on Sources of Figures**

References cited (limited to 21)

1. Rubin, K.H., et al., *Volcanic eruptions in the deep sea.* Oceanography, 2012. **25**(1): p. 142–157.
2. Christeson, G.L., J.A. Goff, and R.S. Reece, *Synthesis of Oceanic Crustal Structure From Two-Dimensional Seismic Profiles.* Reviews of Geophysics, 2019. **57**(2): p. 504-529.

3. Chen, J., J.-A. Olive, and M. Cannat, *Beyond spreading rate: Controls on the thermal regime of mid-ocean ridges.* PNAS, 2023. **120, e2306466120**(45).
4. Chadwick, W.W., Jr., et al., *Voluminous eruption from a zoned magma body after an increase in supply rate at Axial Seamount.* Geophysical Research Letters, 2016. **43**: p. 12063-12070.
5. Soule, S.A., *Mid-Ocean Ridge Volcanism*, in *Encyclopedia of Volcanoes (2nd ed)*, H. Sigurdsson, et al., Editors. 2015, Academic Press: San Diego. p. 395–403.
6. Wu, J.-N., et al., *Extent and Volume of Lava Flows erupted at 9°50'N, East Pacific Rise in 2005–2006 from Autonomous Underwater Vehicle Surveys.* Geochemistry Geophysics Geosystems, 2022. **23, e2021GC010213**.
7. Clague, D.A., et al., *Geologic history of the summit of Axial Seamount, Juan de Fuca Ridge.* Geochemistry Geophysics Geosystems, 2013. **14**(10): p. 4403-4443.
8. Yeo, I., et al., *Eruptive hummocks: Building blocks of the upper ocean crust.* Geology, 2012. **40**(1): p. 91-94.
9. Tucholke, B.E., R. Parnell-Turner, and D.K. Smith, *The global spectrum of seafloor morphology on mid-ocean ridge flanks related to magma supply.* Journal of Geophysical Research: Solid Earth, 2023. **128, e2023JB027367**.
10. Fornari, D.J., et al., *The East Pacific Rise between 9°N and 10°N: Twenty-five years of integrated, multidisciplinary oceanic spreading center studies.* Oceanography, 2012. **25**(1): p. 18–43.
11. Cannat, M., et al., *Modes of seafloor generation at a melt-poor ultraslow-spreading ridge.* Geology, 2006. **34**(7): p. 605–608.
12. Carbotte, S.M., et al., *Tectonic and magmatic segmentation of the Global Ocean Ridge System: a synthesis of observations*, in *Magmatic Rifting and Active Volcanism*, T.J. Wright, et al., Editors. 2015, Geological Society of London.
13. Koepke, J. and C. Zhang, *Axial Melt-Lens Dynamics at Fast Spreading Midocean Ridges*, in *Dynamic Magma Evolution, AGU Geophysical Monograph 254*, F. Vetere, Editor. 2021, American Geophysical Union and John Wiley and Sons, Inc.: Washington, DC and New York, NY. p. 179-206.
14. Rubin, K.H., et al., *Magmatic filtering of mantle compositions at mid-ocean-ridge volcanoes.* Nature Geoscience, 2009. **2**: p. 321-328, doi: 10.1038/NGEO504.
15. Wanless, V.D. and M.D. Behn, *Spreading rate-dependent variations in crystallization along the global mid-ocean ridge system.* Geochemistry Geophysics Geosystems, 2017. **18**: p. 3016–3033.
16. Carbotte, S.M., et al., *Stacked magma lenses beneath mid-ocean ridges: Insights from new seismic observations and synthesis with prior geophysical and geologic findings.* Journal of Geophysical Research: Solid Earth, 2021. **126, e2020JB021434**.
17. Dunn, R.A., *Crust and Lithospheric Structure—Seismic Structure of Mid-Ocean Ridges*, in *Treatise on Geophysics, 2nd edition*, G. Schubert, Editor. 2015, Elsevier: Oxford. p. 419-451.
18. Lissenberg, C.J. and C.J. MacLeod, *A reactive porous flow control on mid-ocean ridge magmatic evolution.* Journal of Petrology, 2016. **57**: p. 2195–2220.
19. Lissenberg, C.J., et al., *A long section of serpentinized depleted mantle peridotite.* Science, 2024. **285**(6709): p. 623-629.
20. Langmuir, C.H. and D.W. Forsyth, *Mantle melting beneath mid-ocean ridges.* Oceanography, 2007. **20**(1): p. 78-89.
21. Katz, R.F., et al., *Physics of Melt Extraction from the Mantle: Speed and Style.* Annual Reviews of Earth and Planetary Science, 2022. **50**: p. 507-540.

SUPPLEMENTARY FILE 1

Figure Captions and Source Information

Figure 1 - Map showing the age of the seafloor and locations of mid-ocean ridges. Relative widths of the 0-10 million year (m.y.) age seafloor (in red) reflects the variation in spreading rate on different mid-ocean ridges. For example, the southern East Pacific Rise spreads at up to 15 cm/yr, whereas the northern Mid-Atlantic Ridge spreads at only 2-3 cm/yr. Figure from Müller et al. (2008) and https://www.ngdc.noaa.gov/mgg/ocean_age/ocean_age_2008.html.

Figure 2. Photos showing the range of submarine lava morphologies; all are video framegrabs from ROV *Jason* dives at Axial Seamount. (a) Pillow lava. (b) Ropy to lineated sheet flow. (c) Collapse area in a lobate sheet flow where the molten interior has drained out below a solid crust. (d) Lava pillars exposed within a collapse area of a lobate sheet flow. (e) Contact between 2015 lava (dark, glassy, upper right) over older seafloor (lighter sedimented pillows, lower left). Photo taken 4 months after the eruption at the thin flow margin where no "eruption mat" formed. (f) Thick "eruption mat" covering a 13-m thick pillow lava flow, only 4 months after it erupted in 2015. The mat is formed by microbial growth where thick lava flows vent warm hydrothermal fluids as they cool. The mat disappears after a few years after the flows have cooled. (Original figure)

Figure 3. Map-scale observations of the seafloor from 1-m-resolution bathymetry collected by AUV. (a) South rift zone of Axial Seamount showing morphology of pillow mounds and ridges. Data from Caress et al., (2012). (b) Northern Gorda Ridge showing contrasting volcanic morphology of high-standing pillow mounds (in yellow and red, above 3050 m depth) and ponded sheet flows with areas of collapse filling low-lying areas (in light to medium blue, below 3050 m depth). Data from Clague et al. (2020). (c) Bathymetry and (d) depth changes before/after the 2011 eruption at Axial Seamount showing channelized sheet flows (black outlines) on gentle slopes near the eruptive vents (white lines) and thicker inflated lobate lava lobes at distal flow fronts. Data from Caress et al., (2012). (e) A 60-m thick lobe of 2015 lava (black outline) erupted from fissures (white lines) on the north rift zone of Axial Seamount. Lobe has pillows on the steep sides, and lobate lava on the top with tumuli and collapse areas. Data from Clague et al. (2017) and Le Saout et al. (2020). (f) Large flow lobe with pillowed margins and lobate top with extensive dendritic collapse areas in the interior of the lobe, south of the caldera at Axial Seamount. Data from Clague et al. (2013). (Original figure)

Figure 4. Variations in ridge crest morphology and segmentation versus spreading rate. (a) Cross-axis depth profiles comparing ridge axis morphology at fast, intermediate, and slow spreading rates. (b) Along-axis depth profiles comparing slow, fast, and superfast spreading ridges. (c) Comparison of ridge segmentation style at fast and slow spreading rate ridges. Figures from Macdonald (2001).

Figure 5. Examples of historical MOR eruptions. (a) Map of new lava erupted in the 2005-2006 eruption on the East Pacific Rise at 9°50'N, outlined in black (original figure, courtesy of Jyun-nai Wu, modified from Wu et al., (2022)). (b) Map of Axial Seamount, Juan de Fuca Ridge, showing outlines of lava flows from the 2011 and 2015 eruptions. Figure from Sigmundsson (2016).

Figure 6. Schematic cross-sections showing the thermal consequences of variable magma supply beneath mid-ocean ridges at different spreading rates (AML = axial melt lens, LVA = low-velocity anomaly). (a) Cross-section of the 6-km thick crust at the fast-spreading East Pacific Rise (EPR) at 9°50'N with a higher magma supply. (b) Cross-section of the 6-km thick crust at a slow-ultraslow spreading segment of the Southwest Indian Ridge (SWIR) with a lower magma supply. However, slow-ultraslow spreading ridges can also undergo periods of higher magmatism, shown by the cross-section in (c) of the magmatically robust but ultra-slow spreading SWIR 50.5°E segment with a 9.5 km-thick crust and a crustal LVA. These differences at the ultraslow-spreading end of the spectrum can be explained by the thermal effects of cyclic changes in melt input, shown by (d) comparing the waxing (top) and waning (bottom) phases of a fluctuating magma supply. Figures from Chen et al. (2023).

References cited

Caress, D. W., D. A. Clague, J. B. Paduan, J. Martin, B. Dreyer, W. W. Chadwick, Jr., A. Denny, and D. S. Kelley (2012), Repeat bathymetric surveys at 1-metre resolution of lava flows erupted at Axial Seamount in April 2011, Nature Geosci., 5(7), 483-488, doi:10.1038/NGEO1496.

Chen, J., J.-A. Olive, and M. Cannat (2023), Beyond spreading rate: Controls on the thermal regime of mid-ocean ridges, PNAS, 120(45), e2306466120, doi:10.1073/pnas.2306466120

Clague, D. A., B. M. Dreyer, J. B. Paduan, J. F. Martin, W. W. Chadwick, Jr., D. W. Caress, R. A. Portner, T. P. Guilderson, M. L. McGann, H. Thomas, D. A. Butterfield, and R. W. Embley (2013), Geologic history of the summit of Axial Seamount, Juan de Fuca Ridge, Geochem. Geophys. Geosyst., 14(10), 4403-4443, doi:10.1002/ggge.20240.

Clague, D. A., J. B. Paduan, D. W. Caress, W. W. Chadwick Jr., M. L. Saout, B. Dreyer, and R. Portner (2017), High-resolution AUV mapping and targeted ROV observations of three historical lava flows at Axial Seamount, Oceanography, 30(4), 82-99, doi:10.5670/oceanog.2017.426.

Clague, D. A., J. B. Paduan, D. W. Caress, J. S. McClain, and R. A. Zierenberg (2020), Lava Flows Erupted in 1996 on North Gorda Ridge Segment and the Geology of the Nearby Sea Cliff Hydrothermal Vent Field From 1-M Resolution AUV Mapping, Front. Mar. Sci., 7(27), doi:10.3389/fmars.2020.00027.

Le Saout, M., D. R. Bohnenstiehl, J. B. Paduan, and D. A. Clague (2020), Quantification of eruption dynamics on the north rift at Axial Seamount, Juan de Fuca Ridge, Geochem. Geophys. Geosyst., 21, e2020GC009136, doi:10.1029/2020GC009136.

Macdonald, K. C. (2001), Mid-Ocean Ridge Tectonics, Volcanism and Geomorphology, in Encyclopedia of Ocean Sciences, edited by J. H. Steele, pp. 1798-1813, Academic Press, San Diego.

Müller, R. D., M. Sdrolias, C. Gaina, and W. R. Roest (2008), Age, spreading rates, and spreading asymmetry of the world's ocean crust, Geochem. Geophys. Geosyst., 9, Q04006, doi:10.1029/2007GC001743.

Sigmundsson, F. (2016), New insights into magma plumbing along rift systems from detailed observations of eruptive behavior at Axial volcano, Geophys. Res. Lett., 43, doi:10.1002/2016GL071884.

Wu, J.-N., R. Parnell-Turner, D. J. Fornari, G. Kurras, N. Berrios-Rivera, T. Barreyre, and J. M. McDermott (2022), Extent and Volume of Lava Flows erupted at 9°50'N, East Pacific Rise in 2005–2006 from Autonomous Underwater Vehicle Surveys, Geochem. Geophys. Geosyst., 23, e2021GC010213, doi:10.1029/2021GC010213.

SUPPLEMENTARY FILE 2

References for Further Reading – six lists, organized by Chapter Section

Section 1 - Introduction

Baker, E. T., W. W. Chadwick, Jr., J. P. Cowen, R. P. Dziak, K. H. Rubin, and D. J. Fornari (2012), Hydrothermal discharge during submarine eruptions: The importance of detection, response, and new technology, Oceanography, 25(1), 128-141, doi: 10.5670/oceanog.2012.11.

Chadwick, W. W., Jr., R. W. Embley, and C. G. Fox (1991), Evidence for volcanic eruption on the southern Juan de Fuca Ridge between 1981 and 1987, Nature, 350, 416-418, doi:10.1038/350416a0.

Chadwick, W. W., Jr., B. P. Paduan, D. A. Clague, B. M. Dreyer, S. G. Merle, A. M. Bobbitt, D. W. Caress, B. Philip, D. S. Kelley, and S. L. Nooner (2016), Voluminous eruption from a zoned magma body after an increase in supply rate at Axial Seamount, Geophys. Res. Lett., 43, 12063-12070, doi:10.1002/2016GL071327.

Chen, J., M. Cannat, C. Tao, D. Sauter, and M. Munschy (2021), 780 thousand years of upper-crustal construction at a melt-rich segment of the ultraslow spreading Southwest Indian Ridge 50°28′E, Journal of Geophysical Research: Solid Earth, 126, e2021JB022152, doi:10.1029/2021JB022152.

Chen, J., J.-A. Olive, and M. Cannat (2023), Beyond spreading rate: Controls on the thermal regime of mid-ocean ridges, PNAS, 120, e2306466120(45), doi:10.1073/pnas.2306466120

Chen, Y. J. (1992), Oceanic crustal thickness versus spreading rate, Geophys. Res. Lett., 19(8), 753–756, doi:10.1029/92GL00161.

Christeson, G. L., J. A. Goff, and R. S. Reece (2019), Synthesis of Oceanic Crustal Structure From Two-Dimensional Seismic Profiles, Rev. Geophys., 57(2), 504-529, doi:10.1029/2019RG000641.

Christie, D. M., and C. R. Fisher (2006), Geological, Biological, Chemical and Physical Interactions in Back-Arc Spreading Systems - An Introduction, in Back Arc Spreading Systems: Geological, Biological, Chemical and Physical Interactions, edited by D. M. Christie, et al., pp. 1-4, American Geophysical Union, Washington, DC.

Colman, A., J. M. Sinton, S. M. White, J. T. McClinton, J. A. Bowles, K. H. Rubin, M. D. Behn, B. Cushman, D. E. Eason, T. K. P. Gregg, K. Grönvold, S. Hidalgo, J. Howell, O. Neill, and C. Russo (2012), Effects of variable magma supply on mid-ocean ridge eruptions: Constraints from mapped lava flow fields along the Galápagos Spreading Center, Geochem. Geophys. Geosyst., 13, Q08014, doi:08010.01029/02012GC004163

Crisp, J. A. (1984), Rates of magma emplacement and volcanic output, J. Volcanol. Geotherm. Res., 20, 177-211

Dziak, R. P., and C. G. Fox (1999), The January 1998 earthquake swarm at Axial Volcano, Juan de Fuca Ridge: Hydroacoustic evidence of seafloor volcanic activity, Geophys. Res. Lett., 26(23), 3429-3432

Dziak, R. P., D. R. Bohnenstiehl, and D. K. Smith (2012), Hydroacoustic monitoring of oceanic spreading centers: Past, present, and future, Oceanography, 25(1), 116–127, doi: 10.5670/oceanog.2012.10.

Fox, C. G., W. W. Chadwick, Jr., and R. W. Embley (1992), Detection of changes in ridge-crest morphology using repeated multibeam sonar surveys, Journal of Geophysical Research: Solid Earth, 97, 11149-11162, doi:10.1029/92JB00601.

Hannington, M. D. (2011), Comments on what processes at mid-ocean ridges tell us about volcanogenic massive sulfide deposits, Mineralium Deposita, 45(5-6), 659-663

Haymon, R. M., D. J. Fornari, K. L. Von Damn, M. D. Lilley, M. R. Perfit, J. M. Edmond, W. C. Shanks, R. A. Lutz, J. M. Grebmeier, S. Carbotte, D. Wright, E. McLaughlin, M. Smith, N. Beedle, and E. Olson (1993), Volcanic eruption of the mid-ocean ridge along the East Pacific Rise crest at 9° 45-52'N: Direct submersible observations of seafloor phenomena associated with an eruption event in April 1991, Earth Planet. Sci. Lett., 119, 85-101

Kelley, D. S., J. R. Delaney, and S. K. Juniper (2014), Establishing a new era of submarine volcanic observatories: Cabling Axial Seamount and the Endeavour Segment of the Juan de Fuca Ridge, Mar. Geol., 352, 426-450, doi:10.1016/j.margeo.2014.03.010.

Le Saout, M., F. M. v. d. Zwan, C. K. Schiebener, and N. Augustin (2023), Magmatism at an ultra-slow spreading rift: high-resolution geomorphological studies of a Red Sea Rift segment in Hadarba Deep, Front. Mar. Sci., 10, 1273574, doi:10.3389/fmars.2023.1273574.

Macdonald, K. C. (2001), Mid-Ocean Ridge Tectonics, Volcanism and Geomorphology, in Encyclopedia of Ocean Sciences, edited by J. H. Steele, pp. 1798-1813, Academic Press, San Diego.

Miller, K. A., K. F. Thompson, P. Johnston, and D. Santillo (2018), An Overview of Seabed Mining Including the Current State of Development, Environmental Impacts, and Knowledge Gaps, Front. Mar. Sci., 4(418), 1-24, doi:10.3389/fmars.2017.00418.

Müller, R. D., M. Sdrolias, C. Gaina, and W. R. Roest (2008), Age, spreading rates, and spreading asymmetry of the world's ocean crust, Geochem. Geophys. Geosyst., 9, Q04006, doi:10.1029/2007GC001743.

Nooner, S. L., and W. W. Chadwick, Jr. (2016), Inflation-predictable behavior and co-eruption deformation at Axial Seamount, Science, 354(6318), 1399-1403, doi:10.1126/science.aah4666.

Perfit, M. R., and W. W. Chadwick, Jr. (1998), Magmatism at mid-ocean ridges: Constraints from volcanological and geochemical investigations, in Faulting and Magmatism at Mid-Ocean Ridges, edited by W. R. Buck, et al., pp. 59-116, American Geophysical Union, Washington DC.

Qin, R., and W. R. Buck (2008), Why meter-wide dikes at oceanic spreading centers, Earth Planet. Sci. Lett., 265(3-4), 466-474, doi:10.1016/j.epsl.2007.10.044.

Rubin, K. H., S. A. Soule, W. W. Chadwick, Jr., D. J. Fornari, D. A. Clague, R. W. Embley, E. T. Baker, M. R. Perfit, D. W. Caress, and R. P. Dziak (2012), Volcanic eruptions in the deep sea, Oceanography, 25(1), 142–157, doi:10.5670/oceanog.2012.12.

Rubin, K. H. (2016), Mid-ocean Ridge Magmatism and Volcanism, in Encyclopedia of Marine Geosciences, edited by J. Harff, et al., pp. 501-513, Springer Dordrecht, Heidelberg, New York, London.

Soule, S. A., D. J. Fornari, M. R. Perfit, and K. H. Rubin (2007), New insights into mid-ocean ridge volcanic processes from the 2005–2006 eruption of the East Pacific Rise, 9°46′N–9°56′N, Geology, 35(12), 1079-1082

Soule, S. A. (2015), Mid-Ocean Ridge Volcanism, in Encyclopedia of Volcanoes (2nd ed), edited by H. Sigurdsson, et al., pp. 395–403, Academic Press, San Diego.

Tolstoy, M., J. P. Cowen, E. T. Baker, D. J. Fornari, K. H. Rubin, T. M. Shank, F. Waldhauser, D. R. Bohnenstiehl, D. W. Forsyth, R. C. Holmes, B. Love, M. R. Perfit, R. T. Weekly, S. A. Soule, and B. Glazer (2006), A sea-floor spreading event captured by seismometers, Science, 314, 1920-1922

Van Dover, C. L., S. Arnaud-Haond, M. Gianni, S. Helmreich, J. A. Huber, A. L. Jaeckel, A. Metaxas, L. H. Pendleton, S. Petersen, E. Ramirez-Llodra, P. E. Steinberg, V. Tunnicliffe, and H. Yamamoto (2018), Scientific rationale and international obligations for protection of active hydrothermal vent ecosystems from deep-sea mining, Marine Policy, 90, 20-28, doi:10.1016/j.marpol.2018.01.020.

Wedding, L. M., S. M. Reiter, C. R. Smith, K. M. Gjerde, J. N. Kittinger, A. M. Friedlander, S. D. Gaines, M. R. Clark, A. M. Thurnherr, S. M. Hardy, and L. B. Crowder (2015), Managing mining of the deep seabed, Science, 349(6244), 144-145, doi:10.1126/science.aac6647.

Wilcock, W. S. D., M. Tolstoy, F. Waldhauser, C. Garcia, Y. J. Tan, D. R. Bohnenstiehl, J. Caplan-Auerbach, R. P. Dziak, A. F. Arnulf, and M. E. Mann (2016), Seismic constraints on caldera dynamics from the 2015 Axial Seamount eruption, Science, 354(6318), 1395-1399, doi:10.1126/science.aah5563.

Section 2 - Mid-Ocean Ridge Eruptions

Caress, D. W., D. A. Clague, J. B. Paduan, J. Martin, B. Dreyer, W. W. Chadwick, Jr., A. Denny, and D. S. Kelley (2012), Repeat bathymetric surveys at 1-metre resolution of lava flows erupted at Axial Seamount in April 2011, Nature Geosci., 5(7), 483-488, doi:10.1038/NGEO1496.

Cas, R. A. F., and J. M. Simmons (2018), Why Deep-Water Eruptions Are So Different From Subaerial Eruptions, Front. Ear. Sci., 6:198, doi:10.3389/feart.2018.00198.

Chadwick, W. W., Jr. (2003), Quantitative constraints on the growth of submarine lava pillars from a monitoring instrument that was caught in a lava flow, Journal of Geophysical Research: Solid Earth, 108, 2534(B11), doi:10.1029/2003JB002422.

Chadwick, W. W., Jr., D. A. Clague, R. W. Embley, M. R. Perfit, D. A. Butterfield, D. W. Caress, J. B. Paduan, J. F. Martin, P. Sasnett, S. G. Merle, and A. M. Bobbitt (2013), The 1998 eruption of Axial Seamount: New Insights on submarine lava flow emplacement from high-resolution mapping, Geochemistry, Geophysics, and Geosystems, 14(10), 3939-3968, doi:10.1002/ggge.20202.

Chadwick, W. W., Jr., B. P. Paduan, D. A. Clague, B. M. Dreyer, S. G. Merle, A. M. Bobbitt, D. W. Caress, B. Philip, D. S. Kelley, and S. L. Nooner (2016), Voluminous eruption from a zoned magma body after an increase in supply rate at Axial Seamount, Geophys. Res. Lett., 43, 12063-12070, doi:10.1002/2016GL071327.

Chen, J., M. Cannat, C. Tao, D. Sauter, and M. Munschy (2021), 780 thousand years of upper-crustal construction at a melt-rich segment of the ultraslow spreading Southwest Indian Ridge 50°28′E, Journal of Geophysical Research: Solid Earth, 126, e2021JB022152, doi:10.1029/2021JB022152.

Clague, D. A., A. S. Davis, and J. E. Dixon (2003), Submarine Strombolian eruptions on the Gorda mid-ocean ridge, in Explosive Subaqueous Volcanism, edited by J. D. L. White, et al., pp. 111-128, American Geophysical Union, Washington DC.

Clague, D. A., J. B. Paduan, and A. S. Davis (2009), Widespread strombolian eruptions of mid-ocean ridge basalt, J. Volcanol. Geotherm. Res., 180, 171-188, doi:110.1016/j.jvolgeores.2008.1008.1007

Clague, D. A., B. M. Dreyer, J. B. Paduan, J. F. Martin, W. W. Chadwick, Jr., D. W. Caress, R. A. Portner, T. P. Guilderson, M. L. McGann, H. Thomas, D. A. Butterfield, and R. W. Embley (2013), Geologic history of the summit of Axial Seamount, Juan de Fuca Ridge, Geochem. Geophys. Geosyst., 14(10), 4403-4443, doi:10.1002/ggge.20240.

Clague, D. A., J. B. Paduan, D. W. Caress, W. W. Chadwick Jr., M. L. Saout, B. Dreyer, and R. Portner (2017), High-resolution AUV mapping and targeted ROV observations of three historical lava flows at Axial Seamount, Oceanography, 30(4), 82-99, doi:10.5670/oceanog.2017.426.

Clague, D. A., J. B. Paduan, B. M. Dreyer, W. W. Chadwick Jr., K. R. Rubin, M. R. Perfit, and A. T. Fundis (2018), Chemical variations in the 1998, 2011, and 2015 lava flows from Axial Seamount, Juan de Fuca Ridge: Cooling during ascent, lateral transport, and flow, Geochem. Geophys. Geosyst., 19, 2915-2933, doi:10.1029/2018GC007708.

Deschamps, A., C. Grigné, M. Le Saout, S. A. Soule, P. Allemand, B. Van Vliet Lanoe, and F. Floc'h (2014), Morphology and dynamics of inflated subaqueous basaltic lava flows, Geochem. Geophys. Geosyst., 15, 2128-2150, doi:10.1002/2014GC005274.

Fox, C. G., W. W. Chadwick, Jr., and R. W. Embley (2001), Direct observation of a submarine volcanic eruption from a sea-floor instrument caught in a lava flow, Nature, 412, 727-729, doi:10.1038/35089066.

Fundis, A. T., S. A. Soule, D. J. Fornari, and M. R. Perfit (2010), Paving the seafloor: Volcanic emplacement processes during the 2005-2006 eruptions at the fast spreading East Pacific Rise, 9°50'N, Geochem. Geophys. Geosyst., 11(8), Q08024, doi:08010.01029/02010GC003058, doi:10.1029/2010GC003058.

Gregg, T. K. P., and J. H. Fink (1995), Quantification of submarine lava-flow morphology through analog experiments, Geology, 23(1), 73-76

Gregg, T. K. P., and W. W. Chadwick, Jr. (1996), Submarine lava-flow inflation: A model for the formation of lava pillars, Geology, 24(11), 981-984, doi:10.1130/0091-7613(1996)024<0981:SLFIAM>2.3.CO;2.

Gregg, T. K. P., D. J. Fornari, M. R. Perfit, R. M. Haymon, and J. H. Fink (1996), Rapid emplacement of a mid-ocean ridge lava flow on the East Pacific Rise at 9° 46'-51'N, Earth Planet. Sci. Lett., 144, E1-E7

Griffiths, R. W., and J. H. Fink (1992), Solidification and morphology of submarine lavas: A dependence on extrusion rate, J. Geophys. Res., 97, 19729-19737

Haymon, R. M., D. J. Fornari, K. L. Von Damn, M. D. Lilley, M. R. Perfit, J. M. Edmond, W. C. Shanks, R. A. Lutz, J. M. Grebmeier, S. Carbotte, D. Wright, E. McLaughlin, M. Smith, N. Beedle, and E. Olson (1993), Volcanic eruption of the mid-ocean ridge along the East Pacific Rise crest at 9° 45-52'N: Direct submersible observations of seafloor phenomena associated with an eruption event in April 1991, Earth Planet. Sci. Lett., 119, 85-101

Helo, C., M. A. Longpre, N. Shimizu, D. A. Clague, and J. Stix (2011), Explosive eruptions at mid-ocean ridges driven by CO2-rich magmas, Nature Geosci., 4, 260-263, doi: 10.1038/NGEO1104.

Le Saout, M., D. R. Bohnenstiehl, J. B. Paduan, and D. A. Clague (2020), Quantification of eruption dynamics on the north rift at Axial Seamount, Juan de Fuca Ridge, Geochem. Geophys. Geosyst., 21, e2020GC009136, doi:10.1029/2020GC009136.

Le Saout, M., F. M. v. d. Zwan, C. K. Schiebener, and N. Augustin (2023), Magmatism at an ultra-slow spreading rift: high-resolution geomorphological studies of a Red Sea Rift segment in Hadarba Deep, Front. Mar. Sci., 10, 1273574, doi:10.3389/fmars.2023.1273574.

McClinton, T., S. M. White, A. Colman, and J. M. Sinton (2013), Reconstructing lava flow emplacement processes at the hotspot-affected Galápagos Spreading Center, 95°W and 92°W, Geochem. Geophys. Geosyst., 14(8), 2731–2756, doi:10.1002/ggge.20157.

Perfit, M. R., J. R. Cann, D. J. Fornari, J. L. Engels, D. K. Smith, W. I. Ridley, and M. H. Edwards (2003), Interaction of sea water and lava during submarine eruptions at mid-ocean ridges, Nature, 426, 62-65

Pontbriand, C. W., S. A. Soule, R. A. Sohn, S. E. Humphris, C. Kunz, H. Singh, K. Nakamura, M. Jakobsson, and T. Shank (2012), Effusive and explosive volcanism on the ultraslow-spreading Gakkel Ridge, 85°E, Geochem. Geophys. Geosyst., 13, Q10005, doi:10010.11029/12012GC004187

Portner, R. A., D. A. Clague, C. Helo, B. M. Dreyer, and J. B. Paduan (2015), Contrasting styles of deep-marine pyroclastic eruptions revealed from Axial Seamount push core records, Earth Planet. Sci. Lett., 423, 219-231, doi:10.1016/j.epsl.2015.03.043.

Schlindwein, V., and C. Riedel (2010), Location and source mechanism of sound signals at Gakkel ridge, Arctic Ocean: Submarine Strombolian activity in the 1999–2001 volcanic episode, Geochem. Geophys. Geosyst., 11, Q01002, doi:10.1029/2009GC002706.

Sinton, J. M., E. Bergmanis, K. Rubin, R. Batiza, T. K. P. Gregg, K. Gronvold, K. C. Macdonald, and S. M. White (2002), Volcanic eruptions on mid-ocean ridges: New evidence from the superfast spreading East Pacific Rise, 17°-19°S, J. Geophys. Res., 107(B6), doi: 10.1029/2000JB000090

Smith, D. K., and J. R. Cann (1990), Hundreds of small volcanoes on the median valley floor of the Mid-Atlantic Ridge at 24-30°N, Nature, 348(6297), 152-155

Sohn, R. A., C. Willis, S. E. Humphris, T. M. Shank, H. Singh, H. N. Edmonds, C. Kunz, U. Hedman, E. Helmke, M. Jakuba, B. Liljebladh, J. Linder, C. Murphy, K. Nakamura, T. Sato, V. Schlindwein, C. Stranne, M. Tausenfreund, L. Upchurch, P. Winsor, M. Jakobsson, and S. Soule (2008), Explosive volcanism on the ultraslow-spreading Gakkel ridge, Arctic Ocean, Nature, 453, 1236-1238

Soule, S. A., D. J. Fornari, M. R. Perfit, and K. H. Rubin (2007), New insights into mid-ocean ridge volcanic processes from the 2005–2006 eruption of the East Pacific Rise, 9°46′N–9°56′N, Geology, 35(12), 1079-1082

Tan, Y. J., M. Tolstoy, F. Waldhauser, and W. Wilcock (2016), Dynamics of a seafloor-spreading episode at the East Pacific Rise, Nature, 540, 261–265, doi:10.1038/nature20116.

Wu, J.-N., R. Parnell-Turner, D. J. Fornari, G. Kurras, N. Berrios-Rivera, T. Barreyre, and J. M. McDermott (2022), Extent and Volume of Lava Flows erupted at 9°50'N, East Pacific Rise in 2005–2006 from Autonomous Underwater Vehicle Surveys, Geochem. Geophys. Geosyst., 23, e2021GC010213, doi:10.1029/2021GC010213.

Yeo, I., R. C. Searle, K. L. Achenbach, T. P. Le Bas, and B. J. Murton (2012), Eruptive hummocks: Building blocks of the upper ocean crust, Geology, 40(1), 91-94

Yeo, I. (2016), Axial Volcanic Ridges, in Encyclopedia of Marine Geosciences, edited by J. Harff, et al., pp. 36-40, Springer Dordrecht, Heidelberg, New York, London.

Yeo, I. A., D. A. Clague, J. F. Martin, J. B. Paduan, and D. W. Caress (2013), Preeruptive flow focussing in dikes feeding historical pillow ridges on the Juan de Fuca and Gorda Ridges, Geochem. Geophys. Geosyst., 14(9), 3586–3599, doi:10.1002/ggge.20210.

Section 3 - Ridge-Axis Morphology and Segmentation

Cannat, M., C. Rommevaux-Jestin, and H. Fujimoto (2003), Melt supply variations to a magma-poor ultra-slow spreading ridge (Southwest Indian Ridge 61° to 69°E), Geochemistry, Geophysics, Geosystems, 4(8), 9104, doi:10.1029/2002GC000480.

Cannat, M., D. Sauter, V. Mendel, E. Ruellan, K. Okino, J. Escartin, V. Combier, and M. Baala (2006), Modes of seafloor generation at a melt-poor ultraslow-spreading ridge, Geology, 34(7), 605–608, doi:10.1130/G22486.1.

Carbotte, S. M., M. Marjanović, H. Carton, J. C. Mutter, J. P. Canales, M. R. Nedimović, S. Han, and M. R. Perfit (2013), Fine-scale segmentation of the crustal magma reservoir beneath the East Pacific Rise, Nature Geosci., 6, 866-870, doi:10.1038/ngeo1933.

Carbotte, S. M., D. K. Smith, M. Cannat, and E. M. Klein (2015), Tectonic and magmatic segmentation of the Global Ocean Ridge System: a synthesis of observations, in Magmatic Rifting and Active Volcanism, edited by T. J. Wright, et al., Geological Society of London.

Escartín, J., C. Mevel, S. Petersen, D. Bonnemains, M. Cannat, M. Andreani, N. Augustin, A. Bezos, V. Chavagnac, Y. Choi, M. Godard, K. Haaga, C. Hamelin, B. Ildefonse, J. Jamieson, B. John, T. Leleu, C. J. MacLeod, M. Massot-Campos, P. Nomikou, J. A. Olive, M. Paquet, C. Rommevaux, M. Rothenbeck, A. Steinfuhrer, M. Tominaga, L. Triebe, R. Campos, N. Gracias, and R. Garcia (2017), Tectonic structure, evolution, and the nature of oceanic core complexes and their detachment fault zones (13°20’ N and 13°30’N, Mid Atlantic Ridge), Geochem. Geophys. Geosyst., 18, 1451–1482, doi:10.1002/2016GC006775.

Fornari, D. J., R. M. Haymon, M. R. Perfit, T. K. P. Gregg, and M. H. Edwards (1998), Axial summit trough of the East Pacific Rise 9°N to 10°N: Geological characteristics and evolution of the axial zone on fast-spreading mid-ocean ridges, J. Geophys. Res., 103(B5), 9827-9855

Fornari, D. J., K. L. V. Damm, J. G. Bryce, J. P. Cowen, V. Ferrini, A. Fundis, M. D. Lilley, G. W. L. III, L. S. Mullineaux, M. R. Perfit, M. F. Meana-Prado, K. H. Rubin, W. E. S. Jr., T. M. Shank, S. A. Soule, M. Tolstoy, and S. M. White (2012), The East Pacific Rise between 9°N and 10°N: Twenty-five years of integrated, multidisciplinary oceanic spreading center studies, Oceanography, 25(1), 18–43, doi: 10.5670/oceanog.2012.02.

Le Saout, M., D. A. Clague, and J. B. Paduan (2019), Evolution of fine-scale segmentation at intermediate-spreading rate ridges, Geochemistry, Geophysics, Geosystems, 20, 3841–3860, doi:10.1029/2019GC008218.

Lin, J., G. M. Purdy, H. Schouten, J.-C. Sempéré, and C. Zervas (1990), Evidence from gravity data for focused magmatic accretion along the Mid-Atlantic Ridge, Nature, 344(6267), 627–632, doi:10.1038/344627a0.

Macdonald, K. C. (1982), Mid-ocean ridges: Fine scale tectonic, volcanic and hydrothermal processes within the plate boundary zone, Rev. Earth Planetary Sci., 10, 155-190

Macdonald, K. C., D. S. Scheirer, and S. M. Carbotte (1991), Mid-ocean ridges: Discontinuities, segments, and giant cracks, Science, 253(5023), 986-994, doi:10.1126/science.253.5023.986.

Marjanović, M., S. M. Carbotte, H. D. Carton, M. R. Nedimović, J. P. Canales, and J. C. Mutter (2018), Crustal Magmatic System Beneath the East Pacific Rise (8°20′ to 10°10′N): Implications for Tectonomagmatic Segmentation and Crustal Melt Transport at Fast-Spreading Ridges, Geochemistry, Geophysics, Geosystems, 19(11), 4584–4611, doi:10.1029/2018GC007590.

Small, C. (1998), Global Systematics of Mid-Ocean Ridge Morphology, in Faulting and Magmatism at Mid-Ocean Ridges, edited by W. R. Buck, et al., pp. 1-25, American Geophysical Union, Washington DC.

Smith, D. K., and J. R. Cann (1993), Building the crust at the Mid-Atlantic Ridge, Nature, 365, 707-715

Smith, D. K., J. R. Cann, and J. Escartín (2006), Widespread active detachment faulting and core complex formation near 13°N on the Mid-Atlantic Ridge, Nature, 442(7101), 440–443, doi:10.1038/nature04950.

Soule, S. A., J. Escartin, and D. J. Fornari (2009), A record of eruption and intrusion at a fast spreading ridge axis: Axial summit trough of the East Pacific Rise at 9–10°, Geochem. Geophys. Geosyst., 10(10), Q10T07, doi:10.1029/2008GC002354

Soule, S. A., and M. R. Perfit (2016), Axial Summit Troughs, in Encyclopedia of Marine Geosciences, edited by J. Harff, et al., pp. 33-35, Springer Dordrecht, Heidelberg, New York, London.

Tucholke, B. E., R. Parnell-Turner, and D. K. Smith (2023), The global spectrum of seafloor morphology on mid-ocean ridge flanks related to magma supply, Journal of Geophysical Research: Solid Earth, 128, e2023JB027367, doi:10.1029/2023JB027367.

Yeo, I., R. C. Searle, K. L. Achenbach, T. P. Le Bas, and B. J. Murton (2012), Eruptive hummocks: Building blocks of the upper ocean crust, Geology, 40(1), 91-94

Yeo, I. (2016), Axial Volcanic Ridges, in Encyclopedia of Marine Geosciences, edited by J. Harff, et al., pp. 36-40, Springer Dordrecht, Heidelberg, New York, London.

Section 4 - Insights From Historical Eruptions

Arnulf, A. F., A. J. Harding, G. M. Kent, S. M. Carbotte, J. P. Canales, and M. R. Nedimovic (2014), Anatomy of an active submarine volcano, Geology, 42(8), 655-658, doi:10.1130/G35629.1.

Arnulf, A. F., A. J. Harding, G. M. Kent, and W. S. D. Wilcock (2018), Structure, seismicity, and accretionary processes at the hotspot-influenced Axial Seamount on the Juan de Fuca Ridge, J. Geophys. Res., 123, doi:10.1029/2017JB015131.

Barreyre, T., R. Parnell-Turner, J.-N. Wu, and D. J. Fornari (2022), Tracking crustal permeability and hydrothermal response during seafloor eruptions at the East Pacific Rise, 9°50'N, Geophys. Res. Lett., 49, e2021GL095459, doi:10.1029/2021GL095459.

Carbotte, S. M., M. Marjanović, H. Carton, J. C. Mutter, J. P. Canales, M. R. Nedimović, S. Han, and M. R. Perfit (2013), Fine-scale segmentation of the crustal magma reservoir beneath the East Pacific Rise, Nature Geosci., 6, 866-870, doi:10.1038/ngeo1933.

Carbotte, S. M., A. F. Arnulf, M. W. Spiegelman, M. Lee, A. J. Harding, G. M. Kent, J. P. Canales, and M. R. Nedimović (2020), Stacked sills forming a deep melt-mush feeder conduit beneath Axial Seamount, Geology, 48, doi:10.1130/G47223.1.

Caress, D. W., D. A. Clague, J. B. Paduan, J. Martin, B. Dreyer, W. W. Chadwick, Jr., A. Denny, and D. S. Kelley (2012), Repeat bathymetric surveys at 1-metre resolution of lava flows erupted at Axial Seamount in April 2011, Nature Geosci., 5(7), 483-488, doi:10.1038/NGEO1496.

Chadwick, J., M. Perfit, I. Ridley, I. Jonasson, G. Kamenov, W. W. Chadwick, Jr., R. Embley, P. Le Roux, and M. Smith (2005), Magmatic effects of the Cobb Hotspot on the Juan de Fuca Ridge, Journal of Geophysical Research: Solid Earth, 110, B03101, doi:10.1029/2003JB002767.

Chadwick, W. W., Jr., D. A. Clague, R. W. Embley, M. R. Perfit, D. A. Butterfield, D. W. Caress, J. B. Paduan, J. F. Martin, P. Sasnett, S. G. Merle, and A. M. Bobbitt (2013), The 1998 eruption of Axial Seamount: New Insights on submarine lava flow emplacement from high-resolution mapping, Geochemistry, Geophysics, and Geosystems, 14(10), 3939-3968, doi:10.1002/ggge.20202.

Chadwick, W. W., Jr., B. P. Paduan, D. A. Clague, B. M. Dreyer, S. G. Merle, A. M. Bobbitt, D. W. Caress, B. Philip, D. S. Kelley, and S. L. Nooner (2016), Voluminous eruption from a zoned magma body after an increase in supply rate at Axial Seamount, Geophys. Res. Lett., 43, 12063-12070, doi:10.1002/2016GL071327.

Chadwick, W. W., Jr., W. S. D. Wilcock, S. L. Nooner, J. W. Beeson, A. M. Sawyer, and T.-K. Lau (2022), Geodetic Monitoring at Axial Seamount Since its 2015 Eruption Reveals a Waning Magma Supply and Tightly Linked Rates of Deformation and Seismicity, Geochem. Geophys. Geosyst., 23(1), e2021GC010153, doi:10.1029/2021GC010153.

Clague, D. A., J. B. Paduan, D. W. Caress, W. W. Chadwick Jr., M. L. Saout, B. Dreyer, and R. Portner (2017), High-resolution AUV mapping and targeted ROV observations of three historical lava flows at Axial Seamount, Oceanography, 30(4), 82-99, doi:10.5670/oceanog.2017.426.

Clague, D. A., J. B. Paduan, B. M. Dreyer, W. W. Chadwick Jr., K. R. Rubin, M. R. Perfit, and A. T. Fundis (2018), Chemical variations in the 1998, 2011, and 2015 lava flows from Axial Seamount, Juan de Fuca Ridge: Cooling during ascent, lateral transport, and flow, Geochem. Geophys. Geosyst., 19, 2915-2933, doi:10.1029/2018GC007708.

Delaney, J. R., D. S. Kelley, M. D. Lilley, D. A. Butterfield, J. A. Baross, W. S. D. Wilcock, R. W. Embley, and M. Summit (1998), The quantum event of oceanic crustal accretion: Impacts of diking at mid-ocean ridges, Science, 281, 222-230

Dziak, R. P., and C. G. Fox (1999), The January 1998 earthquake swarm at Axial Volcano, Juan de Fuca Ridge: Hydroacoustic evidence of seafloor volcanic activity, Geophys. Res. Lett., 26(23), 3429-3432
Fornari, D. J., K. L. V. Damm, J. G. Bryce, J. P. Cowen, V. Ferrini, A. Fundis, M. D. Lilley, G. W. L. III, L. S. Mullineaux, M. R. Perfit, M. F. Meana-Prado, K. H. Rubin, W. E. S. Jr., T. M. Shank, S. A. Soule, M. Tolstoy, and S. M. White (2012), The East Pacific Rise between 9°N and 10°N: Twenty-five years of integrated, multidisciplinary oceanic spreading center studies, Oceanography, 25(1), 18–43, doi: 10.5670/oceanog.2012.02.
Fundis, A. T., S. A. Soule, D. J. Fornari, and M. R. Perfit (2010), Paving the seafloor: Volcanic emplacement processes during the 2005-2006 eruptions at the fast spreading East Pacific Rise, 9°50'N, Geochem. Geophys. Geosyst., 11(8), Q08024, doi:08010.01029/02010GC003058, doi:10.1029/2010GC003058.
Gregg, T. K. P., D. J. Fornari, M. R. Perfit, R. M. Haymon, and J. H. Fink (1996), Rapid emplacement of a mid-ocean ridge lava flow on the East Pacific Rise at 9° 46'-51'N, Earth Planet. Sci. Lett., 144, E1-E7
Haymon, R., D. J. Fornari, M. H. Edwards, S. Carbotte, D. Wright, and K. C. Macdonald (1991), Hydrothermal vent distribution along the East Pacific Rise crest (9°09'-54'N) and its relationship to magmatic and tectonic processes on fast-spreading mid-ocean ridges, Earth Planet. Sci. Lett., 104, 513-534
Le Saout, M., D. R. Bohnenstiehl, J. B. Paduan, and D. A. Clague (2020), Quantification of eruption dynamics on the north rift at Axial Seamount, Juan de Fuca Ridge, Geochem. Geophys. Geosyst., 21, e2020GC009136, doi:10.1029/2020GC009136.
Levy, S., D. R. Bohnenstiehl, P. Sprinkle, M. S. Boettcher, W. S. D. Wilcock, M. Tolstoy, and F. Waldhauser (2018), Mechanics of fault reactivation before, during, and after the 2015 eruption of Axial Seamount, Geology, doi:10.1130/G39978.1.
Marjanović, M., S. M. Carbotte, H. D. Carton, M. R. Nedimović, J. P. Canales, and J. C. Mutter (2018), Crustal Magmatic System Beneath the East Pacific Rise (8°20′ to 10°10′N): Implications for Tectonomagmatic Segmentation and Crustal Melt Transport at Fast-Spreading Ridges, Geochemistry, Geophysics, Geosystems, 19(11), 4584–4611, doi:10.1029/2018GC007590.
Marjanović, M., S. M. Carbotte, A. Stopin, S. C. Singh, R.-É. Plessix, M. Marjanović, M. R. Nedimović, J. P. Canales, H. D. Carton, J. C. Mutter, and J. Escartín (2023), Insights into dike nucleation and eruption dynamics from high-resolution seismic imaging of magmatic system at the East Pacific Rise, Sci. Adv., 9, eadi2698, doi:10.1126/sciadv.adi2698.
Nooner, S. L., and W. W. Chadwick, Jr. (2016), Inflation-predictable behavior and co-eruption deformation at Axial Seamount, Science, 354(6318), 1399-1403, doi:10.1126/science.aah4666.
Soule, S. A., D. J. Fornari, M. R. Perfit, and K. H. Rubin (2007), New insights into mid-ocean ridge volcanic processes from the 2005–2006 eruption of the East Pacific Rise, 9°46′N–9°56′N, Geology, 35(12), 1079-1082
Tan, Y. J., M. Tolstoy, F. Waldhauser, and W. Wilcock (2016), Dynamics of a seafloor-spreading episode at the East Pacific Rise, Nature, 540, 261–265, doi:10.1038/nature20116.
Tan, Y. J., F. Waldhauser, M. Tolstoy, and W. S. D. Wilcock (2019), Axial Seamount: Periodic tidal loading reveals stress dependence of the earthquake size distribution (b value), Earth Planet. Sci. Lett., 512, 39–45
Tolstoy, M., J. P. Cowen, E. T. Baker, D. J. Fornari, K. H. Rubin, T. M. Shank, F. Waldhauser, D. R. Bohnenstiehl, D. W. Forsyth, R. C. Holmes, B. Love, M. R. Perfit, R. T. Weekly, S. A. Soule, and B. Glazer (2006), A sea-floor spreading event captured by seismometers, Science, 314, 1920-1922

Wilcock, W. S. D., M. Tolstoy, F. Waldhauser, C. Garcia, Y. J. Tan, D. R. Bohnenstiehl, J. Caplan-Auerbach, R. P. Dziak, A. F. Arnulf, and M. E. Mann (2016), Seismic constraints on caldera dynamics from the 2015 Axial Seamount eruption, Science, 354(6318), 1395-1399, doi:10.1126/science.aah5563.

Wilcock, W. S. D., R. P. Dziak, M. Tolstoy, W. W. Chadwick Jr., S. L. Nooner, D. R. Bohnenstiehl, J. Caplan-Auerbach, F. Waldhauser, A. Arnulf, C. Baillard, T.-K. Lau, J. H. Haxel, Y. J. Tan, C. Garcia, S. Levy, and M. E. Mann (2018), The recent volcanic history of Axial Seamount: Geophysical insights into past eruption dynamics with an eye toward enhanced observations of future eruptions, Oceanography, 31(1), 114-123, doi:10.5670/oceanog.2018.117.

Wu, J.-N., R. Parnell-Turner, D. J. Fornari, G. Kurras, N. Berrios-Rivera, T. Barreyre, and J. M. McDermott (2022), Extent and Volume of Lava Flows erupted at 9°50'N, East Pacific Rise in 2005–2006 from Autonomous Underwater Vehicle Surveys, Geochem. Geophys. Geosyst., 23, e2021GC010213, doi:10.1029/2021GC010213.

Section 5 - Magma Supply and Storage

Cannat, M. (1996), How thick is the magmatic crust at slow spreading oceanic ridges?, Journal of Geophysical Research Solid Earth, 101(B2), 2847-2857, doi:10.1029/95JB03116.

Carbotte, S. M., M. Marjanović, A. F. Arnulf, M. R. Nedimović, J. P. Canales, and G. M. Arnoux (2021), Stacked magma lenses beneath mid-ocean ridges: Insights from new seismic observations and synthesis with prior geophysical and geologic findings, Journal of Geophysical Research: Solid Earth, 126, e2020JB021434, doi:10.1029/2020JB021434.

Chen, J., M. Cannat, C. Tao, D. Sauter, and M. Munschy (2021), 780 thousand years of upper-crustal construction at a melt-rich segment of the ultraslow spreading Southwest Indian Ridge 50°28′E, Journal of Geophysical Research: Solid Earth, 126, e2021JB022152, doi:10.1029/2021JB022152.

Chen, J., J.-A. Olive, and M. Cannat (2023), Beyond spreading rate: Controls on the thermal regime of mid-ocean ridges, PNAS, 120, e2306466120(45), doi:10.1073/pnas.2306466120

Chen, Y. J. (1992), Oceanic crustal thickness versus spreading rate, Geophys. Res. Lett., 19(8), 753–756, doi:10.1029/92GL00161.

Choi, S., J.-W. Park, J. Kim, J. Oh, C. Park, and S. Han (2024), Melt-rock reaction in the lower oceanic crust and the influence on the evolution of mid-ocean ridge basalts at the Central Indian Ridge (7º50’–8º30’S), J. Petrol., 65, doi:10.1093/petrology/egae057.

Christeson, G. L., J. A. Goff, and R. S. Reece (2019), Synthesis of Oceanic Crustal Structure From Two-Dimensional Seismic Profiles, Rev. Geophys., 57(2), 504-529, doi:10.1029/2019RG000641.

Coogan, L., A. Saunders, P. Kempton, and M. Norry (2000), Evidence from oceanic gabbros for porous melt migration within a crystal mush beneath the Mid-Atlantic Ridge, Geochemsitry Geophysics Geosystems, 1, doi.:10.1029/2000GC000072.

Detrick, R. S., P. Buhl, E. Vera, J. Mutter, J. Orcutt, M. J., and T. Brocher (1987), Multi-channel seismic imaging of a crustal magma chamber along the East Pacific Rise, Nature, 326, 35-41

Detrick, R. S., A. J. Harding, G. M. Kent, J. A. Orcutt, J. C. Mutter, and P. Buhl (1993), Seismic structure of the southern East Pacific Rise, Science, 259, 499-503

Dunn, R. A., D. R. Toomey, and S. C. Solomon (2000), Three-dimensional seismic structure and physical properties of the crust and shallow mantle beneath the East Pacific Rise at 9°30′N, Journal of Geophysical Research Solid Earth, 105(B10), 23537–23556, doi:10.1029/2000JB900210.

Dunn, R. A. (2015), Crust and Lithospheric Structure—Seismic Structure of Mid-Ocean Ridges, in Treatise on Geophysics, 2nd edition, edited by G. Schubert, pp. 419-451, Elsevier, Oxford.

Dunn, R. A., R. Arai, D. E. Eason, J. P. Canales, and R. A. Sohn (2017), Three- dimensional seismic structure of the mid-Atlantic ridge: An investigation of tectonic, magmatic, and hydrothermal processes in the rainbow area, Journal of Geophysical Research: Solid Earth, 122(12), 9580-9602, doi:10.1002/2017JB015051.

Eason, D., and J. Sinton (2006), Origin of high-Al N-MORB by fractional crystallization in the upper mantle beneath the Galápagos Spreading Center,, Earth Planet. Sci. Lett., 252(3-4), 423-436

France, L., B. Ildefonse, and J. Koepke (2009), Interactions between magma and hydrothermal system in Oman ophiolite and in IODP Hole 1256D: Fossilization of a dynamic melt lens at fast spreading ridges, Geochem. Geophys. Geosyst., 10, Q10O19, doi:10.1029/2009GC002652.

France, L., J. Koepke, B. Ildefonse, S. B. Cichy, and F. Deschamps (2010), Hydrous partial melting in the sheeted dike complex at fast spreading ridges: experimental and natural observations, Contrib. Mineral. Petrol. , 160, 683-704, doi:10.1007/s00410-010-0502-6.

Grove, T. L., R. J. Kinzler, and W. B. Bryan (1992), Fractionation of mid-ocean ridge basalt (MORB), in Mantle Flow and Melt Generation at Mid-Ocean Ridges, Geophys. Monogr. Ser., vol. 71, edited by J. P. Morgan, et al., pp. 281-310, AGU, Washington, D. C.

Herzberg, C. (2004), Partial crystallization of mid-ocean ridge basalts in the crust and mantle, J. Petrol., 45, 2389–2405

Humphris, S. E., and J. R. Cann (2000), Constraints on the energy and chemical balances of the modern TAG and ancient Cyprus seafloor sulfide deposits, Journal of Geophysical Research: Solid Earth, 105(B12), 28477-28488, doi:10.1029/2000JB900289.

Klischies, M., S. Petersen, and C. W. Devey (2019), Geological mapping of the Menez Gwen segment at 37°50′N on the Mid-Atlantic Ridge: Implications for accretion mechanisms and associated hydrothermal activity at slow-spreading mid-ocean ridges, Mar. Geol., 412, 107–122, doi:10.1016/j.margeo.2019.03.012.

Koepke, J., D. M. Christie, W. Dziony, F. Holtz, D. Lattard, J. Maclennan, S. Park, B. Scheibner, T. Yamasaki, and S. Yamazaki (2008), Petrography of the dike-gabbro transition at IODP Site 1256 (equatorial Pacific): The evolution of the granoblastic dikes, Geochem. Geophys. Geosyst., 9, doi:10.1029/2008GC001939.

Koepke, J., and C. Zhang (2021), Axial Melt-Lens Dynamics at Fast Spreading Midocean Ridges, in Dynamic Magma Evolution, AGU Geophysical Monograph 254, edited by F. Vetere, pp. 179-206, American Geophysical Union and John Wiley and Sons, Inc., Washington, DC and New York, NY.

Lambart, S., J. M. Koornneef, M. A. Millet, G. R. Davies, M. Cook, and C. J. Lissenberg (2019), Highly heterogeneous depleted mantle recorded in the lower oceanic crust, Nature Geosci., 12(6), 482-486

Lissenberg, C. J., and C. J. MacLeod (2016), A reactive porous flow control on mid-ocean ridge magmatic evolution, J. Petrol., 57, 2195–2220, doi:10.1093/petrology/egw074.

Lissenberg, C. J., C. J. MacLeod, and E. N. Bennett (2019), Consequences of a crystal mush-dominated magma plumbing system: a mid-ocean ridge perspective, Philosophical Transactions of the Royal Society A, 377, 20180014, doi:10.1098/rsta.2018.0014.

Lissenberg, C. J., A. M. McCaig, S. Q. Lang, P. Blum, N. Abe, W. J. Brazelton, R. Coltat, J. R. Deans, K. L. Dickerson, M. Godard, B. E. John, F. Klein, R. Kuehn, K.-Y. Lin, H. Liu, E. L. Lopes, T. Nozaka, A. J. Parsons, V. Pathak, M. K. Reagan, J. A. Robare, I. P. Savov, E. M. Schwarzenbach, O. J. Sissmann, G. Southam, F. Wang, C. G. Wheat, L. Anderson, and S. Treadwell (2024), A long section of serpentinized depleted mantle peridotite, Science, 285(6709), 623-629, doi:10.1126/science.adp1058.

Marjanović, M., S. M. Carbotte, H. Carton, M. R. Nedimovic, J. C. Mutter, and J. P. Canales (2014), A multi-sill magma plumbing system beneath the axis of the East Pacific Rise, Nature Geosci., 7, 825-829, doi:10.1038/NGEO2272.

Marjanović, M., S. M. Carbotte, A. Stopin, S. C. Singh, R.-É. Plessix, M. Marjanović, M. R. Nedimović, J. P. Canales, H. D. Carton, J. C. Mutter, and J. Escartín (2023), Insights into dike nucleation and eruption dynamics from high-resolution seismic imaging of magmatic system at the East Pacific Rise, Sci. Adv., 9, eadi2698, doi:10.1126/sciadv.adi2698.

Rubin, K. H., and J. M. Sinton (2007), Inferences on mid-ocean ridge thermal and magmatic structure from MORB compositions, Earth Planet. Sci. Lett., 260, 257-276

Rubin, K. H., J. M. Sinton, J. Maclennan, and E. Hellebrand (2009), Magmatic filtering of mantle compositions at mid-ocean-ridge volcanoes, Nature Geosci., 2, 321-328, doi: 310.1038/NGEO1504

Singh, S. C., G. M. Kent, J. S. Collier, A. J. Harding, and J. A. Orcutt (1998), Melt to mush variations in crustal magma properties along the ridge crest at the southern East Pacific Rise, Nature, 394(6696), 874–878, doi:10.1038/nature29740.

Sinton, J. M., and R. S. Detrick (1992), Mid-ocean ridge magma chambers, J. Geophys. Res., 97, 197-216

Tominaga, M., D. A. H. Teagle, J. C. Alt, and S. Umino (2009), Determination of the volcanostratigraphy of oceanic crust formed at superfast spreading ridge: Electrofacies analyses of ODP/IODP Hole 1256D, Geochem. Geophys. Geosyst., 10, Q01003, doi:10.1029/2008GC002143.

Tominaga, M., and S. Umino (2010), Lava deposition history in ODP Hole 1256D: Insights from log-based volcanostratigraphy, Geochem. Geophys. Geosyst., 11, Q05003, doi:10.1029/2009GC002933.

Wanless, V. D., and A. M. Shaw (2012), Lower crustal crystallization and melt evolution at mid-ocean ridges, Nature Geosci., 5, 651-655, doi:10.1038/NGEO1552.

Wanless, V. D., A. M. Shaw, M. D. Behn, S. A. Soule, J. Escartín, and C. Hamelin (2015), Magmatic plumbing at Lucky Strike volcano based on olivine-hosted melt inclusion compositions, Geochem. Geophys. Geosyst., 16(1), 126-147

Wanless, V. D., and M. D. Behn (2017), Spreading rate-dependent variations in crystallization along the global mid-ocean ridge system, Geochem. Geophys. Geosyst., 18, 3016–3033, doi:10.1002/2017GC006924.

Section 6 - Mantle Melting Processes

Asimow, P. D., and C. H. Langmuir (2003), The importance of water to oceanic mantle melting regimes, Nature, 421, 815–820

Cannat, M., C. Mevel, M. Maia, C. Deplus, C. Durand, P. Gente, P. Agrinier, A. Belarouchi, G. Dubuisson, E. Humler, and J. Reynolds (1995), Thin crust, ultramafic exposures, and rugged faulting patterns at the Mid-Atlantic Ridge (22°–24°N, Geology, 23(1), 49-52, doi:10.1130/0091-7613(1995)023<0049:tcuear>2.3.co;2.

Carbotte, S. M., C. Small, and K. Donnelly (2004), The influence of ridge migration on the magmatic segmentation of mid-ocean ridges, Nature, 429(6993), 743–746

Chen, Y. J. (1992), Oceanic crustal thickness versus spreading rate, Geophys. Res. Lett., 19(8), 753–756, doi:10.1029/92GL00161.

Choblet, G., and E. M. Parmentier (2001), Mantle upwelling and melting beneath slow spreading centers: effects of variable rheology and melt productivity, Earth Planet. Sci. Lett., 184, 589-604

Christeson, G. L., J. A. Goff, and R. S. Reece (2019), Synthesis of Oceanic Crustal Structure From Two-Dimensional Seismic Profiles, Rev. Geophys., 57(2), 504-529, doi:10.1029/2019RG000641.

Gale, A., C. A. Dalton, C. H. Langmuir, Y. Su, and J.-G.Schilling (2013), The mean composition of ocean ridge basalts, Geochem. Geophys. Geosyst., 14, 489–518

Gregg, P. M., L. B. Hebert, L. G. J. Montési, and R. F. Katz (2012), Geodynamic models of melt generation and extraction at mid-ocean ridges, Oceanography, 25(1), 78–88, doi: 10.5670/oceanog.2012.05.

Katz, R. F. (2010), Porosity-driven convection and asymmetry beneath mid-ocean ridges, Geochemistry, Geophysics, Geosystems, 11(11), doi:10.1029/2010GC003282.

Katz, R. F., D. W. Rees Jones, J. F. Rudge, and T. Keller (2022), Physics of Melt Extraction from the Mantle: Speed and Style, Annual Reviews of Earth and Planetary Science, 50, 507-540, doi:10.1146/annurev-earth-032320-083704.

Lambart, S., J. M. Koornneef, M. A. Millet, G. R. Davies, M. Cook, and C. J. Lissenberg (2019), Highly heterogeneous depleted mantle recorded in the lower oceanic crust, Nature Geosci., 12(6), 482-486

Langmuir, C. H., E. M. Klein, and T. Plank (1992), Petrological systematics of mid-ocean ridge basalts: Constraints on melt generation beneath ocean ridges, in Mantle Flow and Melt Generation at Mid-Ocean Ridges, edited by J. Phipps Morgan, et al., pp. 183–280, American Geophysical Union, Washington, DC.

Langmuir, C. H., and D. W. Forsyth (2007), Mantle melting beneath mid-ocean ridges, Oceanography, 20(1), 78-89

Lissenberg, C. J., A. M. McCaig, S. Q. Lang, P. Blum, N. Abe, W. J. Brazelton, R. Coltat, J. R. Deans, K. L. Dickerson, M. Godard, B. E. John, F. Klein, R. Kuehn, K.-Y. Lin, H. Liu, E. L. Lopes, T. Nozaka, A. J. Parsons, V. Pathak, M. K. Reagan, J. A. Robare, I. P. Savov, E. M. Schwarzenbach, O. J. Sissmann, G. Southam, F. Wang, C. G. Wheat, L. Anderson, and S. Treadwell (2024), A long section of serpentinized depleted mantle peridotite, Science, 285(6709), 623-629, doi:10.1126/science.adp1058.

Liu, M., T. Gerya, and A. B. Rozel (2022), Self-organization of magma supply controls crustal thickness variation and tectonic pattern along melt-poor mid-ocean ridges., Earth Planet. Sci. Lett., 584, 117482

Magde, L. S., and D. W. Sparks (1997), Three-dimensional mantle upwelling, melt generation, and melt migration beneath segment slow spreading ridges, Journal of Geophysical Research: Solid Earth, 102(B9), 20571-20583

Magde, L. S., D. W. Sparks, and R. S. Detrick (1997), The relationship between buoyant mantle flow, melt migration, and gravity bull's eyes at the Mid-Atlantic Ridge between 33º N and 35º N, Earth Planet. Sci. Lett., 148, 59–67

Parmentier, E. M., and J. P. Morgan (1990), The spreading rate dependence of three-dimensional oceanic spreading center structure, Nature, 348, 325–328

Plank, T., and C. H. Langmuir (1992), Effects of melting regime on the composition of the ocean crust, Journal of Geophysical Research: Solid Earth, 97(B13), 19749-19770

Rabinowicz, M., S. Rouzo, J.-C. Sempere, and C. Rosemberg (1993), Three-dimensional mantle flow beneath mid-ocean ridges, J. Geophys. Res., 98, 7851–7869

Rees Jones, D. W., H. Zhang, and R. F. Katz (2021), Magmatic channelization by reactive and shear-driven instabilities at mid-ocean ridges: a combined analysis, Geophys. J. Int., 226, 582–609

Rubin, K. H., J. M. Sinton, J. Maclennan, and E. Hellebrand (2009), Magmatic filtering of mantle compositions at mid-ocean-ridge volcanoes, Nature Geosci., 2, 321-328, doi: 310.1038/NGEO1504

Spiegelman, M., P. Kelemen, and E. Aharonov (2001), Causes and consequences of flow organization during melt transport: the reaction infiltration instability in compactible media, J. Geophys. Res., 106(B2), 2061–2077

Wanless, V. D., and A. M. Shaw (2012), Lower crustal crystallization and melt evolution at mid-ocean ridges, Nature Geosci., 5, 651-655, doi:10.1038/NGEO1552.

Wanless, V. D., A. M. Shaw, M. D. Behn, S. A. Soule, J. Escartín, and C. Hamelin (2015), Magmatic plumbing at Lucky Strike volcano based on olivine-hosted melt inclusion compositions, Geochem. Geophys. Geosyst., 16(1), 126-147

SUPPLEMENTARY FILE 3

References for Further Reading – one list with all references

Arnulf, A. F., A. J. Harding, G. M. Kent, S. M. Carbotte, J. P. Canales, and M. R. Nedimovic (2014), Anatomy of an active submarine volcano, Geology, 42(8), 655-658, doi:10.1130/G35629.1.
Arnulf, A. F., A. J. Harding, G. M. Kent, and W. S. D. Wilcock (2018), Structure, seismicity, and accretionary processes at the hotspot-influenced Axial Seamount on the Juan de Fuca Ridge, J. Geophys. Res., 123, doi:10.1029/2017JB015131.
Asimow, P. D., and C. H. Langmuir (2003), The importance of water to oceanic mantle melting regimes, Nature, 421, 815–820
Baker, E. T., W. W. Chadwick, Jr., J. P. Cowen, R. P. Dziak, K. H. Rubin, and D. J. Fornari (2012), Hydrothermal discharge during submarine eruptions: The importance of detection, response, and new technology, Oceanography, 25(1), 128-141, doi: 10.5670/oceanog.2012.11.
Barreyre, T., R. Parnell-Turner, J.-N. Wu, and D. J. Fornari (2022), Tracking crustal permeability and hydrothermal response during seafloor eruptions at the East Pacific Rise, 9°50'N, Geophys. Res. Lett., 49, e2021GL095459, doi:10.1029/2021GL095459.
Cannat, M., C. Mevel, M. Maia, C. Deplus, C. Durand, P. Gente, P. Agrinier, A. Belarouchi, G. Dubuisson, E. Humler, and J. Reynolds (1995), Thin crust, ultramafic exposures, and rugged faulting patterns at the Mid-Atlantic Ridge (22°–24°N, Geology, 23(1), 49-52, doi:10.1130/0091-7613(1995)023<0049:tcuear>2.3.co;2.
Cannat, M. (1996), How thick is the magmatic crust at slow spreading oceanic ridges?, Journal of Geophysical Research Solid Earth, 101(B2), 2847-2857, doi:10.1029/95JB03116.
Cannat, M., C. Rommevaux-Jestin, and H. Fujimoto (2003), Melt supply variations to a magma-poor ultra-slow spreading ridge (Southwest Indian Ridge 61° to 69°E), Geochemistry, Geophysics, Geosystems, 4(8), 9104, doi:10.1029/2002GC000480.
Cannat, M., D. Sauter, V. Mendel, E. Ruellan, K. Okino, J. Escartin, V. Combier, and M. Baala (2006), Modes of seafloor generation at a melt-poor ultraslow-spreading ridge, Geology, 34(7), 605–608, doi:10.1130/G22486.1.
Carbotte, S. M., C. Small, and K. Donnelly (2004), The influence of ridge migration on the magmatic segmentation of mid-ocean ridges, Nature, 429(6993), 743–746
Carbotte, S. M., M. Marjanović, H. Carton, J. C. Mutter, J. P. Canales, M. R. Nedimović, S. Han, and M. R. Perfit (2013), Fine-scale segmentation of the crustal magma reservoir beneath the East Pacific Rise, Nature Geosci., 6, 866-870, doi:10.1038/ngeo1933.
Carbotte, S. M., D. K. Smith, M. Cannat, and E. M. Klein (2015), Tectonic and magmatic segmentation of the Global Ocean Ridge System: a synthesis of observations, in Magmatic Rifting and Active Volcanism, edited by T. J. Wright, et al., Geological Society of London.
Carbotte, S. M., A. F. Arnulf, M. W. Spiegelman, M. Lee, A. J. Harding, G. M. Kent, J. P. Canales, and M. R. Nedimović (2020), Stacked sills forming a deep melt-mush feeder conduit beneath Axial Seamount, Geology, 48, doi:10.1130/G47223.1.
Carbotte, S. M., M. Marjanović, A. F. Arnulf, M. R. Nedimović, J. P. Canales, and G. M. Arnoux (2021), Stacked magma lenses beneath mid-ocean ridges: Insights from new seismic observations and synthesis with prior geophysical and geologic findings, Journal of Geophysical Research: Solid Earth, 126, e2020JB021434, doi:10.1029/2020JB021434.
Caress, D. W., D. A. Clague, J. B. Paduan, J. Martin, B. Dreyer, W. W. Chadwick, Jr., A. Denny, and D. S. Kelley (2012), Repeat bathymetric surveys at 1-metre resolution of lava flows erupted at Axial Seamount in April 2011, Nature Geosci., 5(7), 483-488, doi:10.1038/NGEO1496.

Cas, R. A. F., and J. M. Simmons (2018), Why Deep-Water Eruptions Are So Different From Subaerial Eruptions, Front. Ear. Sci., 6:198, doi:10.3389/feart.2018.00198.
Chadwick, J., M. Perfit, I. Ridley, I. Jonasson, G. Kamenov, W. W. Chadwick, Jr., R. Embley, P. Le Roux, and M. Smith (2005), Magmatic effects of the Cobb Hotspot on the Juan de Fuca Ridge, Journal of Geophysical Research: Solid Earth, 110, B03101, doi:10.1029/2003JB002767.
Chadwick, W. W., Jr., R. W. Embley, and C. G. Fox (1991), Evidence for volcanic eruption on the southern Juan de Fuca Ridge between 1981 and 1987, Nature, 350, 416-418, doi:10.1038/350416a0.
Chadwick, W. W., Jr. (2003), Quantitative constraints on the growth of submarine lava pillars from a monitoring instrument that was caught in a lava flow, Journal of Geophysical Research: Solid Earth, 108, 2534(B11), doi:10.1029/2003JB002422.
Chadwick, W. W., Jr., D. A. Clague, R. W. Embley, M. R. Perfit, D. A. Butterfield, D. W. Caress, J. B. Paduan, J. F. Martin, P. Sasnett, S. G. Merle, and A. M. Bobbitt (2013), The 1998 eruption of Axial Seamount: New Insights on submarine lava flow emplacement from high-resolution mapping, Geochemistry, Geophysics, and Geosystems, 14(10), 3939-3968, doi:10.1002/ggge.20202.
Chadwick, W. W., Jr., B. P. Paduan, D. A. Clague, B. M. Dreyer, S. G. Merle, A. M. Bobbitt, D. W. Caress, B. Philip, D. S. Kelley, and S. L. Nooner (2016), Voluminous eruption from a zoned magma body after an increase in supply rate at Axial Seamount, Geophys. Res. Lett., 43, 12063-12070, doi:10.1002/2016GL071327.
Chadwick, W. W., Jr., W. S. D. Wilcock, S. L. Nooner, J. W. Beeson, A. M. Sawyer, and T.-K. Lau (2022), Geodetic Monitoring at Axial Seamount Since its 2015 Eruption Reveals a Waning Magma Supply and Tightly Linked Rates of Deformation and Seismicity, Geochem. Geophys. Geosyst., 23(1), e2021GC010153, doi:10.1029/2021GC010153.
Chen, J., M. Cannat, C. Tao, D. Sauter, and M. Munschy (2021), 780 thousand years of upper-crustal construction at a melt-rich segment of the ultraslow spreading Southwest Indian Ridge 50°28′E, Journal of Geophysical Research: Solid Earth, 126, e2021JB022152, doi:10.1029/2021JB022152.
Chen, J., J.-A. Olive, and M. Cannat (2023), Beyond spreading rate: Controls on the thermal regime of mid-ocean ridges, PNAS, 120, e2306466120(45), doi:10.1073/pnas.2306466120
Chen, Y. J. (1992), Oceanic crustal thickness versus spreading rate, Geophys. Res. Lett., 19(8), 753–756, doi:10.1029/92GL00161.
Choblet, G., and E. M. Parmentier (2001), Mantle upwelling and melting beneath slow spreading centers: effects of variable rheology and melt productivity, Earth Planet. Sci. Lett., 184, 589-604
Choi, S., J.-W. Park, J. Kim, J. Oh, C. Park, and S. Han (2024), Melt-rock reaction in the lower oceanic crust and the influence on the evolution of mid-ocean ridge basalts at the Central Indian Ridge (7º50'–8º30'S), J. Petrol., 65, doi:10.1093/petrology/egae057.
Christeson, G. L., J. A. Goff, and R. S. Reece (2019), Synthesis of Oceanic Crustal Structure From Two-Dimensional Seismic Profiles, Rev. Geophys., 57(2), 504-529, doi:10.1029/2019RG000641.
Christie, D. M., and C. R. Fisher (2006), Geological, Biological, Chemical and Physical Interactions in Back-Arc Spreading Systems - An Introduction, in Back Arc Spreading Systems: Geological, Biological, Chemical and Physical Interactions, edited by D. M. Christie, et al., pp. 1-4, American Geophysical Union, Washington, DC.
Clague, D. A., A. S. Davis, and J. E. Dixon (2003), Submarine Strombolian eruptions on the Gorda mid-ocean ridge, in Explosive Subaqueous Volcanism, edited by J. D. L. White, et al., pp. 111-128, American Geophysical Union, Washington DC.

Clague, D. A., J. B. Paduan, and A. S. Davis (2009), Widespread strombolian eruptions of mid-ocean ridge basalt, J. Volcanol. Geotherm. Res., 180, 171-188, doi:110.1016/j.jvolgeores.2008.1008.1007
Clague, D. A., B. M. Dreyer, J. B. Paduan, J. F. Martin, W. W. Chadwick, Jr., D. W. Caress, R. A. Portner, T. P. Guilderson, M. L. McGann, H. Thomas, D. A. Butterfield, and R. W. Embley (2013), Geologic history of the summit of Axial Seamount, Juan de Fuca Ridge, Geochem. Geophys. Geosyst., 14(10), 4403-4443, doi:10.1002/ggge.20240.
Clague, D. A., J. B. Paduan, D. W. Caress, W. W. Chadwick Jr., M. L. Saout, B. Dreyer, and R. Portner (2017), High-resolution AUV mapping and targeted ROV observations of three historical lava flows at Axial Seamount, Oceanography, 30(4), 82-99, doi:10.5670/oceanog.2017.426.
Clague, D. A., J. B. Paduan, B. M. Dreyer, W. W. Chadwick Jr., K. R. Rubin, M. R. Perfit, and A. T. Fundis (2018), Chemical variations in the 1998, 2011, and 2015 lava flows from Axial Seamount, Juan de Fuca Ridge: Cooling during ascent, lateral transport, and flow, Geochem. Geophys. Geosyst., 19, 2915-2933, doi:10.1029/2018GC007708.
Colman, A., J. M. Sinton, S. M. White, J. T. McClinton, J. A. Bowles, K. H. Rubin, M. D. Behn, B. Cushman, D. E. Eason, T. K. P. Gregg, K. Grönvold, S. Hidalgo, J. Howell, O. Neill, and C. Russo (2012), Effects of variable magma supply on mid-ocean ridge eruptions: Constraints from mapped lava flow fields along the Galápagos Spreading Center, Geochem. Geophys. Geosyst., 13, Q08014, doi:08010.01029/02012GC004163
Coogan, L., A. Saunders, P. Kempton, and M. Norry (2000), Evidence from oceanic gabbros for porous melt migration within a crystal mush beneath the Mid-Atlantic Ridge, Geochemsitry Geophysics Geosystems, 1, doi.:10.1029/2000GC000072.
Crisp, J. A. (1984), Rates of magma emplacement and volcanic output, J. Volcanol. Geotherm. Res., 20, 177-211
Delaney, J. R., D. S. Kelley, M. D. Lilley, D. A. Butterfield, J. A. Baross, W. S. D. Wilcock, R. W. Embley, and M. Summit (1998), The quantum event of oceanic crustal accretion: Impacts of diking at mid-ocean ridges, Science, 281, 222-230
Deschamps, A., C. Grigné, M. Le Saout, S. A. Soule, P. Allemand, B. Van Vliet Lanoe, and F. Floc'h (2014), Morphology and dynamics of inflated subaqueous basaltic lava flows, Geochem. Geophys. Geosyst., 15, 2128-2150, doi:10.1002/2014GC005274.
Detrick, R. S., P. Buhl, E. Vera, J. Mutter, J. Orcutt, M. J., and T. Brocher (1987), Multi-channel seismic imaging of a crustal magma chamber along the East Pacific Rise, Nature, 326, 35-41
Detrick, R. S., A. J. Harding, G. M. Kent, J. A. Orcutt, J. C. Mutter, and P. Buhl (1993), Seismic structure of the southern East Pacific Rise, Science, 259, 499-503
Dunn, R. A., D. R. Toomey, and S. C. Solomon (2000), Three-dimensional seismic structure and physical properties of the crust and shallow mantle beneath the East Pacific Rise at 9°30′N, Journal of Geophysical Research Solid Earth, 105(B10), 23537–23556, doi:10.1029/2000JB900210.
Dunn, R. A. (2015), Crust and Lithospheric Structure—Seismic Structure of Mid-Ocean Ridges, in Treatise on Geophysics, 2nd edition, edited by G. Schubert, pp. 419-451, Elsevier, Oxford.
Dunn, R. A., R. Arai, D. E. Eason, J. P. Canales, and R. A. Sohn (2017), Three- dimensional seismic structure of the mid-Atlantic ridge: An investigation of tectonic, magmatic, and hydrothermal processes in the rainbow area, Journal of Geophysical Research: Solid Earth, 122(12), 9580-9602, doi:10.1002/2017JB015051.
Dziak, R. P., and C. G. Fox (1999), The January 1998 earthquake swarm at Axial Volcano, Juan de Fuca Ridge: Hydroacoustic evidence of seafloor volcanic activity, Geophys. Res. Lett., 26(23), 3429-3432

Dziak, R. P., D. R. Bohnenstiehl, and D. K. Smith (2012), Hydroacoustic monitoring of oceanic spreading centers: Past, present, and future, Oceanography, 25(1), 116–127, doi: 10.5670/oceanog.2012.10.

Eason, D., and J. Sinton (2006), Origin of high-Al N-MORB by fractional crystallization in the upper mantle beneath the Galápagos Spreading Center,, Earth Planet. Sci. Lett., 252(3-4), 423-436

Escartín, J., C. Mevel, S. Petersen, D. Bonnemains, M. Cannat, M. Andreani, N. Augustin, A. Bezos, V. Chavagnac, Y. Choi, M. Godard, K. Haaga, C. Hamelin, B. Ildefonse, J. Jamieson, B. John, T. Leleu, C. J. MacLeod, M. Massot-Campos, P. Nomikou, J. A. Olive, M. Paquet, C. Rommevaux, M. Rothenbeck, A. Steinfuhrer, M. Tominaga, L. Triebe, R. Campos, N. Gracias, and R. Garcia (2017), Tectonic structure, evolution, and the nature of oceanic core complexes and their detachment fault zones (13°20' N and 13°30'N, Mid Atlantic Ridge), Geochem. Geophys. Geosyst., 18, 1451–1482, doi:10.1002/2016GC006775.

Fornari, D. J., R. M. Haymon, M. R. Perfit, T. K. P. Gregg, and M. H. Edwards (1998), Axial summit trough of the East Pacific Rise 9°N to 10°N: Geological characteristics and evolution of the axial zone on fast-spreading mid-ocean ridges, J. Geophys. Res., 103(B5), 9827-9855

Fornari, D. J., K. L. V. Damm, J. G. Bryce, J. P. Cowen, V. Ferrini, A. Fundis, M. D. Lilley, G. W. L. III, L. S. Mullineaux, M. R. Perfit, M. F. Meana-Prado, K. H. Rubin, W. E. S. Jr., T. M. Shank, S. A. Soule, M. Tolstoy, and S. M. White (2012), The East Pacific Rise between 9°N and 10°N: Twenty-five years of integrated, multidisciplinary oceanic spreading center studies, Oceanography, 25(1), 18–43, doi: 10.5670/oceanog.2012.02.

Fox, C. G., W. W. Chadwick, Jr., and R. W. Embley (1992), Detection of changes in ridge-crest morphology using repeated multibeam sonar surveys, Journal of Geophysical Research: Solid Earth, 97, 11149-11162, doi:10.1029/92JB00601.

Fox, C. G., W. W. Chadwick, Jr., and R. W. Embley (2001), Direct observation of a submarine volcanic eruption from a sea-floor instrument caught in a lava flow, Nature, 412, 727-729, doi:10.1038/35089066.

France, L., B. Ildefonse, and J. Koepke (2009), Interactions between magma and hydrothermal system in Oman ophiolite and in IODP Hole 1256D: Fossilization of a dynamic melt lens at fast spreading ridges, Geochem. Geophys. Geosyst., 10, Q10O19, doi:10.1029/2009GC002652.

France, L., J. Koepke, B. Ildefonse, S. B. Cichy, and F. Deschamps (2010), Hydrous partial melting in the sheeted dike complex at fast spreading ridges: experimental and natural observations, Contrib. Mineral. Petrol. , 160, 683-704, doi:10.1007/s00410-010-0502-6.

Fundis, A. T., S. A. Soule, D. J. Fornari, and M. R. Perfit (2010), Paving the seafloor: Volcanic emplacement processes during the 2005-2006 eruptions at the fast spreading East Pacific Rise, 9°50'N, Geochem. Geophys. Geosyst., 11(8), Q08024, doi:08010.01029/02010GC003058, doi:10.1029/2010GC003058.

Gale, A., C. A. Dalton, C. H. Langmuir, Y. Su, and J.-G.Schilling (2013), The mean composition of ocean ridge basalts, Geochem. Geophys. Geosyst., 14, 489–518

Gregg, P. M., L. B. Hebert, L. G. J. Montési, and R. F. Katz (2012), Geodynamic models of melt generation and extraction at mid-ocean ridges, Oceanography, 25(1), 78–88, doi: 10.5670/oceanog.2012.05.

Gregg, T. K. P., and J. H. Fink (1995), Quantification of submarine lava-flow morphology through analog experiments, Geology, 23(1), 73-76

Gregg, T. K. P., and W. W. Chadwick, Jr. (1996), Submarine lava-flow inflation: A model for the formation of lava pillars, Geology, 24(11), 981-984, doi:10.1130/0091-7613(1996)024<0981:SLFIAM>2.3.CO;2.

Gregg, T. K. P., D. J. Fornari, M. R. Perfit, R. M. Haymon, and J. H. Fink (1996), Rapid emplacement of a mid-ocean ridge lava flow on the East Pacific Rise at 9° 46'-51'N, Earth Planet. Sci. Lett., 144, E1-E7

Griffiths, R. W., and J. H. Fink (1992), Solidification and morphology of submarine lavas: A dependence on extrusion rate, J. Geophys. Res., 97, 19729-19737

Grove, T. L., R. J. Kinzler, and W. B. Bryan (1992), Fractionation of mid-ocean ridge basalt (MORB), in Mantle Flow and Melt Generation at Mid-Ocean Ridges, Geophys. Monogr. Ser., vol. 71, edited by J. P. Morgan, et al., pp. 281-310, AGU, Washington, D. C.

Hannington, M. D. (2011), Comments on what processes at mid-ocean ridges tell us about volcanogenic massive sulfide deposits, Mineralium Deposita, 45(5-6), 659-663

Haymon, R., D. J. Fornari, M. H. Edwards, S. Carbotte, D. Wright, and K. C. Macdonald (1991), Hydrothermal vent distribution along the East Pacific Rise crest (9°09'-54'N) and its relationship to magmatic and tectonic processes on fast-spreading mid-ocean ridges, Earth Planet. Sci. Lett., 104, 513-534

Haymon, R. M., D. J. Fornari, K. L. Von Damn, M. D. Lilley, M. R. Perfit, J. M. Edmond, W. C. Shanks, R. A. Lutz, J. M. Grebmeier, S. Carbotte, D. Wright, E. McLaughlin, M. Smith, N. Beedle, and E. Olson (1993), Volcanic eruption of the mid-ocean ridge along the East Pacific Rise crest at 9° 45-52'N: Direct submersible observations of seafloor phenomena associated with an eruption event in April 1991, Earth Planet. Sci. Lett., 119, 85-101

Helo, C., M. A. Longpre, N. Shimizu, D. A. Clague, and J. Stix (2011), Explosive eruptions at mid-ocean ridges driven by CO2-rich magmas, Nature Geosci., 4, 260-263, doi: 10.1038/NGEO1104.

Herzberg, C. (2004), Partial crystallization of mid-ocean ridge basalts in the crust and mantle, J. Petrol., 45, 2389–2405

Humphris, S. E., and J. R. Cann (2000), Constraints on the energy and chemical balances of the modern TAG and ancient Cyprus seafloor sulfide deposits, Journal of Geophysical Research: Solid Earth, 105(B12), 28477-28488, doi:10.1029/2000JB900289.

Katz, R. F. (2010), Porosity-driven convection and asymmetry beneath mid-ocean ridges, Geochemistry, Geophysics, Geosystems, 11(11), doi:10.1029/2010GC003282.

Katz, R. F., D. W. Rees Jones, J. F. Rudge, and T. Keller (2022), Physics of Melt Extraction from the Mantle: Speed and Style, Annual Reviews of Earth and Planetary Science, 50, 507-540, doi:10.1146/annurev-earth-032320-083704.

Kelley, D. S., J. R. Delaney, and S. K. Juniper (2014), Establishing a new era of submarine volcanic observatories: Cabling Axial Seamount and the Endeavour Segment of the Juan de Fuca Ridge, Mar. Geol., 352, 426-450, doi:10.1016/j.margeo.2014.03.010.

Klischies, M., S. Petersen, and C. W. Devey (2019), Geological mapping of the Menez Gwen segment at 37°50′N on the Mid-Atlantic Ridge: Implications for accretion mechanisms and associated hydrothermal activity at slow-spreading mid-ocean ridges, Mar. Geol., 412, 107–122, doi:10.1016/j.margeo.2019.03.012.

Koepke, J., D. M. Christie, W. Dziony, F. Holtz, D. Lattard, J. Maclennan, S. Park, B. Scheibner, T. Yamasaki, and S. Yamazaki (2008), Petrography of the dike-gabbro transition at IODP Site 1256 (equatorial Pacific): The evolution of the granoblastic dikes, Geochem. Geophys. Geosyst., 9, doi:10.1029/2008GC001939.

Koepke, J., and C. Zhang (2021), Axial Melt-Lens Dynamics at Fast Spreading Midocean Ridges, in Dynamic Magma Evolution, AGU Geophysical Monograph 254, edited by F. Vetere, pp. 179-206, American Geophysical Union and John Wiley and Sons, Inc., Washington, DC and New York, NY.

Lambart, S., J. M. Koornneef, M. A. Millet, G. R. Davies, M. Cook, and C. J. Lissenberg (2019), Highly heterogeneous depleted mantle recorded in the lower oceanic crust, Nature Geosci., 12(6), 482-486

Langmuir, C. H., E. M. Klein, and T. Plank (1992), Petrological systematics of mid-ocean ridge basalts: Constraints on melt generation beneath ocean ridges, in Mantle Flow and Melt Generation at Mid-Ocean Ridges, edited by J. Phipps Morgan, et al., pp. 183–280, American Geophysical Union, Washington, DC.

Langmuir, C. H., and D. W. Forsyth (2007), Mantle melting beneath mid-ocean ridges, Oceanography, 20(1), 78-89

Le Saout, M., D. A. Clague, and J. B. Paduan (2019), Evolution of fine-scale segmentation at intermediate-spreading rate ridges, Geochemistry, Geophysics, Geosystems, 20, 3841–3860, doi:10.1029/2019GC008218.

Le Saout, M., D. R. Bohnenstiehl, J. B. Paduan, and D. A. Clague (2020), Quantification of eruption dynamics on the north rift at Axial Seamount, Juan de Fuca Ridge, Geochem. Geophys. Geosyst., 21, e2020GC009136, doi:10.1029/2020GC009136.

Le Saout, M., F. M. v. d. Zwan, C. K. Schiebener, and N. Augustin (2023), Magmatism at an ultra-slow spreading rift: high-resolution geomorphological studies of a Red Sea Rift segment in Hadarba Deep, Front. Mar. Sci., 10, 1273574, doi:10.3389/fmars.2023.1273574.

Levy, S., D. R. Bohnenstiehl, P. Sprinkle, M. S. Boettcher, W. S. D. Wilcock, M. Tolstoy, and F. Waldhauser (2018), Mechanics of fault reactivation before, during, and after the 2015 eruption of Axial Seamount, Geology, doi:10.1130/G39978.1.

Lin, J., G. M. Purdy, H. Schouten, J.-C. Sempéré, and C. Zervas (1990), Evidence from gravity data for focused magmatic accretion along the Mid-Atlantic Ridge, Nature, 344(6267), 627–632, doi:10.1038/344627a0.

Lissenberg, C. J., and C. J. MacLeod (2016), A reactive porous flow control on mid-ocean ridge magmatic evolution, J. Petrol., 57, 2195–2220, doi:10.1093/petrology/egw074.

Lissenberg, C. J., C. J. MacLeod, and E. N. Bennett (2019), Consequences of a crystal mush-dominated magma plumbing system: a mid-ocean ridge perspective, Philosophical Transactions of the Royal Society A, 377, 20180014, doi:10.1098/rsta.2018.0014.

Lissenberg, C. J., A. M. McCaig, S. Q. Lang, P. Blum, N. Abe, W. J. Brazelton, R. Coltat, J. R. Deans, K. L. Dickerson, M. Godard, B. E. John, F. Klein, R. Kuehn, K.-Y. Lin, H. Liu, E. L. Lopes, T. Nozaka, A. J. Parsons, V. Pathak, M. K. Reagan, J. A. Robare, I. P. Savov, E. M. Schwarzenbach, O. J. Sissmann, G. Southam, F. Wang, C. G. Wheat, L. Anderson, and S. Treadwell (2024), A long section of serpentinized depleted mantle peridotite, Science, 285(6709), 623-629, doi:10.1126/science.adp1058.

Liu, M., T. Gerya, and A. B. Rozel (2022), Self-organization of magma supply controls crustal thickness variation and tectonic pattern along melt-poor mid-ocean ridges., Earth Planet. Sci. Lett., 584, 117482

Macdonald, K. C. (1982), Mid-ocean ridges: Fine scale tectonic, volcanic and hydrothermal processes within the plate boundary zone, Rev. Earth Planetary Sci., 10, 155-190

Macdonald, K. C., D. S. Scheirer, and S. M. Carbotte (1991), Mid-ocean ridges: Discontinuities, segments, and giant cracks, Science, 253(5023), 986-994, doi:10.1126/science.253.5023.986.

Macdonald, K. C. (2001), Mid-Ocean Ridge Tectonics, Volcanism and Geomorphology, in Encyclopedia of Ocean Sciences, edited by J. H. Steele, pp. 1798-1813, Academic Press, San Diego.

Magde, L. S., and D. W. Sparks (1997), Three-dimensional mantle upwelling, melt generation, and melt migration beneath segment slow spreading ridges, Journal of Geophysical Research: Solid Earth, 102(B9), 20571-20583

Magde, L. S., D. W. Sparks, and R. S. Detrick (1997), The relationship between buoyant mantle flow, melt migration, and gravity bull's eyes at the Mid-Atlantic Ridge between 33º N and 35º N, Earth Planet. Sci. Lett., 148, 59–67

Marjanović, M., S. M. Carbotte, H. Carton, M. R. Nedimovic, J. C. Mutter, and J. P. Canales (2014), A multi-sill magma plumbing system beneath the axis of the East Pacific Rise, Nature Geosci., 7, 825-829, doi:10.1038/NGEO2272.
Marjanović, M., S. M. Carbotte, H. D. Carton, M. R. Nedimović, J. P. Canales, and J. C. Mutter (2018), Crustal Magmatic System Beneath the East Pacific Rise (8°20′ to 10°10′N): Implications for Tectonomagmatic Segmentation and Crustal Melt Transport at Fast-Spreading Ridges, Geochemistry, Geophysics, Geosystems, 19(11), 4584–4611, doi:10.1029/2018GC007590.
Marjanović, M., S. M. Carbotte, A. Stopin, S. C. Singh, R.-É. Plessix, M. Marjanović, M. R. Nedimović, J. P. Canales, H. D. Carton, J. C. Mutter, and J. Escartín (2023), Insights into dike nucleation and eruption dynamics from high-resolution seismic imaging of magmatic system at the East Pacific Rise, Sci. Adv., 9, eadi2698, doi:10.1126/sciadv.adi2698.
McClinton, T., S. M. White, A. Colman, and J. M. Sinton (2013), Reconstructing lava flow emplacement processes at the hotspot-affected Galápagos Spreading Center, 95°W and 92°W, Geochem. Geophys. Geosyst., 14(8), 2731–2756, doi:10.1002/ggge.20157.
Miller, K. A., K. F. Thompson, P. Johnston, and D. Santillo (2018), An Overview of Seabed Mining Including the Current State of Development, Environmental Impacts, and Knowledge Gaps, Front. Mar. Sci., 4(418), 1-24, doi:10.3389/fmars.2017.00418.
Müller, R. D., M. Sdrolias, C. Gaina, and W. R. Roest (2008), Age, spreading rates, and spreading asymmetry of the world’s ocean crust, Geochem. Geophys. Geosyst., 9, Q04006, doi:10.1029/2007GC001743.
Nooner, S. L., and W. W. Chadwick, Jr. (2016), Inflation-predictable behavior and co-eruption deformation at Axial Seamount, Science, 354(6318), 1399-1403, doi:10.1126/science.aah4666.
Parmentier, E. M., and J. P. Morgan (1990), The spreading rate dependence of three-dimensional oceanic spreading center structure, Nature, 348, 325–328
Perfit, M. R., and W. W. Chadwick, Jr. (1998), Magmatism at mid-ocean ridges: Constraints from volcanological and geochemical investigations, in Faulting and Magmatism at Mid-Ocean Ridges, edited by W. R. Buck, et al., pp. 59-116, American Geophysical Union, Washington DC.
Perfit, M. R., J. R. Cann, D. J. Fornari, J. L. Engels, D. K. Smith, W. I. Ridley, and M. H. Edwards (2003), Interaction of sea water and lava during submarine eruptions at mid-ocean ridges, Nature, 426, 62-65
Plank, T., and C. H. Langmuir (1992), Effects of melting regime on the composition of the ocean crust, Journal of Geophysical Research: Solid Earth, 97(B13), 19749-19770
Pontbriand, C. W., S. A. Soule, R. A. Sohn, S. E. Humphris, C. Kunz, H. Singh, K. Nakamura, M. Jakobsson, and T. Shank (2012), Effusive and explosive volcanism on the ultraslow-spreading Gakkel Ridge, 85°E, Geochem. Geophys. Geosyst., 13, Q10005, doi:10010.11029/12012GC004187
Portner, R. A., D. A. Clague, C. Helo, B. M. Dreyer, and J. B. Paduan (2015), Contrasting styles of deep-marine pyroclastic eruptions revealed from Axial Seamount push core records, Earth Planet. Sci. Lett., 423, 219-231, doi:10.1016/j.epsl.2015.03.043.
Qin, R., and W. R. Buck (2008), Why meter-wide dikes at oceanic spreading centers, Earth Planet. Sci. Lett., 265(3-4), 466-474, doi:10.1016/j.epsl.2007.10.044.
Rabinowicz, M., S. Rouzo, J.-C. Sempere, and C. Rosemberg (1993), Three-dimensional mantle flow beneath mid-ocean ridges, J. Geophys. Res., 98, 7851–7869
Rees Jones, D. W., H. Zhang, and R. F. Katz (2021), Magmatic channelization by reactive and shear-driven instabilities at mid-ocean ridges: a combined analysis, Geophys. J. Int., 226, 582–609
Rubin, K. H., and J. M. Sinton (2007), Inferences on mid-ocean ridge thermal and magmatic structure from MORB compositions, Earth Planet. Sci. Lett., 260, 257-276

Rubin, K. H., J. M. Sinton, J. Maclennan, and E. Hellebrand (2009), Magmatic filtering of mantle compositions at mid-ocean-ridge volcanoes, Nature Geosci., 2, 321-328, doi: 310.1038/NGEO1504
Rubin, K. H., S. A. Soule, W. W. Chadwick, Jr., D. J. Fornari, D. A. Clague, R. W. Embley, E. T. Baker, M. R. Perfit, D. W. Caress, and R. P. Dziak (2012), Volcanic eruptions in the deep sea, Oceanography, 25(1), 142–157, doi:10.5670/oceanog.2012.12.
Rubin, K. H. (2016), Mid-ocean Ridge Magmatism and Volcanism, in Encyclopedia of Marine Geosciences, edited by J. Harff, et al., pp. 501-513, Springer Dordrecht, Heidelberg, New York, London.
Schlindwein, V., and C. Riedel (2010), Location and source mechanism of sound signals at Gakkel ridge, Arctic Ocean: Submarine Strombolian activity in the 1999–2001 volcanic episode, Geochem. Geophys. Geosyst., 11, Q01002, doi:10.1029/2009GC002706.
Singh, S. C., G. M. Kent, J. S. Collier, A. J. Harding, and J. A. Orcutt (1998), Melt to mush variations in crustal magma properties along the ridge crest at the southern East Pacific Rise, Nature, 394(6696), 874–878, doi:10.1038/nature29740.
Sinton, J. M., and R. S. Detrick (1992), Mid-ocean ridge magma chambers, J. Geophys. Res., 97, 197-216
Sinton, J. M., E. Bergmanis, K. Rubin, R. Batiza, T. K. P. Gregg, K. Gronvold, K. C. Macdonald, and S. M. White (2002), Volcanic eruptions on mid-ocean ridges: New evidence from the superfast spreading East Pacific Rise, 17°-19°S, J. Geophys. Res., 107(B6), doi: 10.1029/2000JB000090
Small, C. (1998), Global Systematics of Mid-Ocean Ridge Morphology, in Faulting and Magmatism at Mid-Ocean Ridges, edited by W. R. Buck, et al., pp. 1-25, American Geophysical Union, Washington DC.
Smith, D. K., and J. R. Cann (1990), Hundreds of small volcanoes on the median valley floor of the Mid-Atlantic Ridge at 24-30°N, Nature, 348(6297), 152-155
Smith, D. K., and J. R. Cann (1993), Building the crust at the Mid-Atlantic Ridge, Nature, 365, 707-715
Smith, D. K., J. R. Cann, and J. Escartín (2006), Widespread active detachment faulting and core complex formation near 13°N on the Mid-Atlantic Ridge, Nature, 442(7101), 440–443, doi:10.1038/nature04950.
Sohn, R. A., C. Willis, S. E. Humphris, T. M. Shank, H. Singh, H. N. Edmonds, C. Kunz, U. Hedman, E. Helmke, M. Jakuba, B. Liljebladh, J. Linder, C. Murphy, K. Nakamura, T. Sato, V. Schlindwein, C. Stranne, M. Tausenfreund, L. Upchurch, P. Winsor, M. Jakobsson, and S. Soule (2008), Explosive volcanism on the ultraslow-spreading Gakkel ridge, Arctic Ocean, Nature, 453, 1236-1238
Soule, S. A., D. J. Fornari, M. R. Perfit, and K. H. Rubin (2007), New insights into mid-ocean ridge volcanic processes from the 2005–2006 eruption of the East Pacific Rise, 9°46′N–9°56′N, Geology, 35(12), 1079-1082
Soule, S. A., J. Escartin, and D. J. Fornari (2009), A record of eruption and intrusion at a fast spreading ridge axis: Axial summit trough of the East Pacific Rise at 9–10°, Geochem. Geophys. Geosyst., 10(10), Q10T07, doi:10.1029/2008GC002354
Soule, S. A. (2015), Mid-Ocean Ridge Volcanism, in Encyclopedia of Volcanoes (2nd ed), edited by H. Sigurdsson, et al., pp. 395–403, Academic Press, San Diego.
Soule, S. A., and M. R. Perfit (2016), Axial Summit Troughs, in Encyclopedia of Marine Geosciences, edited by J. Harff, et al., pp. 33-35, Springer Dordrecht, Heidelberg, New York, London.
Spiegelman, M., P. Kelemen, and E. Aharonov (2001), Causes and consequences of flow organization during melt transport: the reaction infiltration instability in compactible media, J. Geophys. Res., 106(B2), 2061–2077

Tan, Y. J., M. Tolstoy, F. Waldhauser, and W. Wilcock (2016), Dynamics of a seafloor-spreading episode at the East Pacific Rise, Nature, 540, 261–265, doi:10.1038/nature20116.

Tan, Y. J., F. Waldhauser, M. Tolstoy, and W. S. D. Wilcock (2019), Axial Seamount: Periodic tidal loading reveals stress dependence of the earthquake size distribution (b value), Earth Planet. Sci. Lett., 512, 39–45

Tolstoy, M., J. P. Cowen, E. T. Baker, D. J. Fornari, K. H. Rubin, T. M. Shank, F. Waldhauser, D. R. Bohnenstiehl, D. W. Forsyth, R. C. Holmes, B. Love, M. R. Perfit, R. T. Weekly, S. A. Soule, and B. Glazer (2006), A sea-floor spreading event captured by seismometers, Science, 314, 1920-1922

Tominaga, M., D. A. H. Teagle, J. C. Alt, and S. Umino (2009), Determination of the volcanostratigraphy of oceanic crust formed at superfast spreading ridge: Electrofacies analyses of ODP/IODP Hole 1256D, Geochem. Geophys. Geosyst., 10, Q01003, doi:10.1029/2008GC002143.

Tominaga, M., and S. Umino (2010), Lava deposition history in ODP Hole 1256D: Insights from log-based volcanostratigraphy, Geochem. Geophys. Geosyst., 11, Q05003, doi:10.1029/2009GC002933.

Tucholke, B. E., R. Parnell-Turner, and D. K. Smith (2023), The global spectrum of seafloor morphology on mid-ocean ridge flanks related to magma supply, Journal of Geophysical Research: Solid Earth, 128, e2023JB027367, doi:10.1029/2023JB027367.

Van Dover, C. L., S. Arnaud-Haond, M. Gianni, S. Helmreich, J. A. Huber, A. L. Jaeckel, A. Metaxas, L. H. Pendleton, S. Petersen, E. Ramirez-Llodra, P. E. Steinberg, V. Tunnicliffe, and H. Yamamoto (2018), Scientific rationale and international obligations for protection of active hydrothermal vent ecosystems from deep-sea mining, Marine Policy, 90, 20-28, doi:10.1016/j.marpol.2018.01.020.

Wanless, V. D., and A. M. Shaw (2012), Lower crustal crystallization and melt evolution at mid-ocean ridges, Nature Geosci., 5, 651-655, doi:10.1038/NGEO1552.

Wanless, V. D., A. M. Shaw, M. D. Behn, S. A. Soule, J. Escartín, and C. Hamelin (2015), Magmatic plumbing at Lucky Strike volcano based on olivine-hosted melt inclusion compositions, Geochem. Geophys. Geosyst., 16(1), 126-147

Wanless, V. D., and M. D. Behn (2017), Spreading rate-dependent variations in crystallization along the global mid-ocean ridge system, Geochem. Geophys. Geosyst., 18, 3016–3033, doi:10.1002/2017GC006924.

Wedding, L. M., S. M. Reiter, C. R. Smith, K. M. Gjerde, J. N. Kittinger, A. M. Friedlander, S. D. Gaines, M. R. Clark, A. M. Thurnherr, S. M. Hardy, and L. B. Crowder (2015), Managing mining of the deep seabed, Science, 349(6244), 144-145, doi:10.1126/science.aac6647.

Wilcock, W. S. D., M. Tolstoy, F. Waldhauser, C. Garcia, Y. J. Tan, D. R. Bohnenstiehl, J. Caplan-Auerbach, R. P. Dziak, A. F. Arnulf, and M. E. Mann (2016), Seismic constraints on caldera dynamics from the 2015 Axial Seamount eruption, Science, 354(6318), 1395-1399, doi:10.1126/science.aah5563.

Wilcock, W. S. D., R. P. Dziak, M. Tolstoy, W. W. Chadwick Jr., S. L. Nooner, D. R. Bohnenstiehl, J. Caplan-Auerbach, F. Waldhauser, A. Arnulf, C. Baillard, T.-K. Lau, J. H. Haxel, Y. J. Tan, C. Garcia, S. Levy, and M. E. Mann (2018), The recent volcanic history of Axial Seamount: Geophysical insights into past eruption dynamics with an eye toward enhanced observations of future eruptions, Oceanography, 31(1), 114-123, doi:10.5670/oceanog.2018.117.

Wu, J.-N., R. Parnell-Turner, D. J. Fornari, G. Kurras, N. Berrios-Rivera, T. Barreyre, and J. M. McDermott (2022), Extent and Volume of Lava Flows erupted at 9°50'N, East Pacific Rise in 2005–2006 from Autonomous Underwater Vehicle Surveys, Geochem. Geophys. Geosyst., 23, e2021GC010213, doi:10.1029/2021GC010213.

Yeo, I., R. C. Searle, K. L. Achenbach, T. P. Le Bas, and B. J. Murton (2012), Eruptive hummocks: Building blocks of the upper ocean crust, Geology, 40(1), 91-94
Yeo, I. (2016), Axial Volcanic Ridges, in Encyclopedia of Marine Geosciences, edited by J. Harff, et al., pp. 36-40, Springer Dordrecht, Heidelberg, New York, London.
Yeo, I. A., D. A. Clague, J. F. Martin, J. B. Paduan, and D. W. Caress (2013), Preeruptive flow focussing in dikes feeding historical pillow ridges on the Juan de Fuca and Gorda Ridges, Geochem. Geophys. Geosyst., 14(9), 3586–3599, doi:10.1002/ggge.20210.